

Mixed variable structural optimization using mixed variable system Monte Carlo tree search formulation

Fu-Yao Ko¹ · Katsuyuki Suzuki¹ · Kazuo Yonekura¹

Abstract

A novel method called mixed variable system Monte Carlo tree search (MVSMCTS) formulation is presented for optimization problems considering various types of variables with single and mixed continuous-discrete system. This method utilizes a reinforcement learning algorithm with improved Monte Carlo tree search (IMCTS) formulation. For sizing and shape optimization of truss structures, the design variables are the cross-sectional areas of the members and the nodal coordinates of the joints. MVSMCTS incorporates update process and accelerating technique for continuous variable and combined scheme for single and mixed system. Update process indicates that once a solution is determined by MCTS with automatic mesh generation in continuous space, it is used as the initial solution for next search tree. The search region should be expanded from the mid-point, which is the design variable for initial state. Accelerating technique is developed by decreasing the range of search region and the width of search tree based on the number of meshes during update process. Combined scheme means that various types of variables are coupled in only one search tree. Through several examples, it is demonstrated that this framework is suitable for mixed variable structural optimization. Moreover, the agent can find optimal solution in a reasonable time, stably generates an optimal design, and is applicable for practical engineering problems.

Keywords Truss structures · Combined sizing and shape optimization · Mixed continuous-discrete system · Reinforcement learning · Mixed system Monte Carlo tree search formulation

1 Introduction

Structural optimization has received considerable attention during the past decades due to limited material resources (Vanderplaats 1982). For sizing and shape optimization of truss structures, it becomes necessary to optimize cross-sectional areas of members and nodal coordinates of joints simultaneously (Kunar and Chan 1976; Topping 1983; Kuritz and Fleury 1989). From a weight-saving aspect, this optimization problem can provide more reduction in weight than purity sizing optimization (Kirsch and Topping 1992; Gholizadeh 2013). However, this problem is considered to be more challenging because the two types of variables involved are of fundamentally different nature.

Combining these may produce a different rate of convergence and induce the problem to be ill-conditioning (Vanderplaats and Moses 1972; Lipson and Gwin 1977; Wu and Chow 1995). To overcome the difficulties, two main classes of optimization methods have been published using mathematical programming (Yonekura and Kanno 2010; Kanno and Fujita 2018) and metaheuristics (Vargas et al. 2019; Lagaros et al. 2023).

Reinforcement learning (RL) is a branch of machine learning that aims to train an action taker called agent to take actions to maximize the cumulative numerical reward signal (Sutton and Barto 2018). Markov decision process (MDP) is the most basic theoretical model and mathematical expression for RL problems. In recent years, Q-learning-based RL approaches have been successfully used for structural design problems (Hayashi and Ohsaki 2020; Hayashi and Ohsaki 2022; Kupwiwat et al. 2024). It can be applied to structural optimization problems where it is not easy to find the optimal solutions beforehand. Moreover, RL approach does not require desired outputs as training data. However, the most significant limitation of this method is the high computational cost for training the agent. (Hayashi and Ohsaki 2020).

Recently, a Monte Carlo tree search-based RL algorithm is proposed to solve truss optimization problems. MCTS is a best-first search algorithm to solve sequential decision problems. MCTS starts with a single root node and expands the search tree that relies on random simulations rather than on full exploration. MCTS can select the optimal decision in the large search space with very little domain-specific prior knowledge. However, a huge amount of memory usage and computational resource is required to construct a search tree (Browne et al. 2012; Zuccotto et al. 2024).

A novel MCTS-based RL algorithm (Luo et al. 2022a; Luo et al. 2022b) was developed to generate optimal truss layout considering sizing, shape, and topology. Continuous design variables are considered in this study. Moreover, an RL algorithm using improved Monte Carlo tree search (IMCTS) formulation (Ko et al. 2024) was presented for discrete optimum design of truss structures. It utilizes the search tree with multiple root nodes. This formulation includes update process and accelerating technique for discrete variable, the best reward, and terminal condition. The agent is trained to minimize the weight of the truss subjected to stress and displacement constraints. The numerical results demonstrate that IMCTS formulation can find optimal solution at a low computational cost, stably generates an optimal design, and is applicable for practical engineering problems and multi-objective optimization of structures. However, IMCTS formulation is only applied to structural optimization problems considering one type of variable with discrete cases.

In this paper, mixed variable system Monte Carlo tree search (MVSMCTS) formulation based on IMCTS formulation is developed to deal with both sizing and shape variable. MVSMCTS formulation incorporates update process and accelerating

technique for continuous variable and combined scheme for single and mixed continuous-discrete system. A united computational framework of update process is formed for truss design with both discrete variable and continuous one. The difference is that the solution is found by MCTS with automatic mesh generation in continuous space. Combined scheme indicates that various types of variables are considered in only one search tree. Through several numerical examples, it is demonstrated that MVSMCTS is suitable for mixed variable structural optimization. Also, the agent can find optimal solution with low computational cost, stably generates an optimal design, and is applicable for practical engineering problems.

2 A brief review on formulation of sizing-shape truss optimization problems and IMCTS formulation for discrete truss optimization

MVSMCTS formulation is applicable for mixed variable structural optimization. The optimal design of truss structures for sizing and shape is used as an example in this study. Therefore, this section first briefly reviews its formulation. Then, an RL algorithm using IMCTS formulation for discrete optimum design of truss structures is recalled because its concepts will be utilized in the proposed algorithm.

2.1 Formulation of the sizing and shape optimization of truss structures

The aim of the mixed variable structural optimization is to minimize the weight of structures considering various types of variables while satisfying design constraints. In this class of optimization problems, there are two types of design variables: sizing variable (cross-sectional areas of members) and shape variable (coordinates of nodes). The optimization problem can be described in mathematical formulations as below:

$$\mathbf{X} = (X_1, X_2, \dots, X_{i_X}, \dots, X_{g_X}) \quad (1a)$$

$$\mathbf{Y} = (Y_1, Y_2, \dots, Y_{i_Y}, \dots, Y_{g_Y}) \quad (1b)$$

$$\text{Find } X_{i_X} \in \mathbf{D}_{X,i_X} = \{(d_{X,i_X})_1, (d_{X,i_X})_2, \dots, (d_{X,i_X})_h, \dots, (d_{X,i_X})_{b_X}\} \quad (1c)$$

$$Y_{i_Y} \in \mathbf{D}_{Y,i_Y} = \{(d_{Y,i_Y})_1, (d_{Y,i_Y})_2, \dots, (d_{Y,i_Y})_h, \dots, (d_{Y,i_Y})_{b_Y}\} \quad (1d)$$

$$X_{i_X, \min} \leq X_{i_X} \leq X_{i_X, \max} \quad (1e)$$

$$Y_{i_Y, \min} \leq Y_{i_Y} \leq Y_{i_Y, \max} \quad (1f)$$

$$\text{Minimize } W(\mathbf{X}, \mathbf{Y}) = \rho \sum_{i_X=1}^{g_X} \left(X_{i_X} \sum_{j=1}^{m_{i_X}} L_{i_X,j}(Y_{i_Y}) \right) \quad (1g)$$

where \mathbf{X} and \mathbf{Y} are the sizing vector containing the cross-sectional areas and the shape vector containing the coordinates of nodes; X_{i_X} is the cross-sectional area of the members belonging to group i_X ; Y_{i_Y} is the coordinate of the node i_Y ; X_{i_X} and Y_{i_Y} are selected from a list of available discrete values or can be any continuous value; g_X and

g_Y are the number of design variables for sizing and shape; \mathbf{D}_{X,i_X} and \mathbf{D}_{Y,i_Y} are the lists including all available discrete values arranged in ascending sequences for X_{i_X} and Y_{i_Y} ; $(d_{X,i_X})_h$ and $(d_{Y,i_Y})_h$ are the elements in lists \mathbf{D}_{X,i_X} and \mathbf{D}_{Y,i_Y} ; h is the index of permissive discrete variable; b_X and b_Y are the number of available variables for X_{i_X} and Y_{i_Y} ; $X_{i_X,\min}$ and $X_{i_X,\max}$ are the lower and upper limit for X_{i_X} ; $Y_{i_Y,\min}$ and $Y_{i_Y,\max}$ are the lower and upper limit for Y_{i_Y} ; $W(\mathbf{X}, \mathbf{Y})$ is the objective function measuring the weight of the truss; ρ is the material density; m_{i_X} is the number of members in group i_X ; and $L_{i_X,j}(Y_{i_Y})$ is the length of the member j in group i_X , which is the function of Y_{i_Y} . The constraints can be stated as follows:

$$\mathbf{K}(\mathbf{X}, \mathbf{Y})\mathbf{u} = \mathbf{F} \quad (2a)$$

$$\mathbf{F} = (F_1^x, F_1^y, F_1^z, F_2^x, F_2^y, F_2^z, \dots, F_k^x, F_k^y, F_k^z, \dots) \quad (2b)$$

$$\varepsilon_{i_X,j} = \mathbf{B}_{i_X,j} \mathbf{u}_{i_X,j} \quad (2c)$$

$$\mathbf{B}_{i_X,j} = (-\mathbf{e}_{i_X,j}^{\text{tr}} \quad \mathbf{e}_{i_X,j}^{\text{tr}}) \quad (2d)$$

$$\text{Subject to } \mathbf{u}_{i_X,j} = (\mathbf{u}_{i_X,j}^1 \quad \mathbf{u}_{i_X,j}^2)^{\text{tr}} \quad (2e)$$

$$\sigma_{i_X,j} = \frac{E}{L_{i_X,j}} \varepsilon_{i_X,j} \quad (2f)$$

$$\sigma_{\min} \leq \sigma_{i_X,j} \leq \sigma_{\max}, i_X = 1, 2, \dots, g_X, j = 1, 2, \dots, m_{i_X} \quad (2g)$$

$$\delta_{\min} \leq \delta_k \leq \delta_{\max}, k = 1, 2, \dots, c \quad (2h)$$

where $\mathbf{K}(\mathbf{X}, \mathbf{Y})$ is the global stiffness matrix of the entire truss; \mathbf{u} is a vector with the displacements of the non-suppressed nodes of the entire truss; \mathbf{F} is a vector with the given external forces at these nodes; F_k^x , F_k^y , and F_k^z are the x , y , and z components of external force acting on node k ; $\varepsilon_{i_X,j}$ is the elongation of the member; $\mathbf{e}_{i_X,j}$ is a unit vector along the member so that it points from node 1 to node 2; $\mathbf{u}_{i_X,j}$ is a vector with the displacements of the end points of the member; tr in the superscript of a given vector is the transpose operator; E is the modulus of elasticity; and c is the number of nodes in the truss. From Eqs. 2d and 2e, the stress $\sigma_{i,j}$ in each member of the truss is compared with σ_{\max} and σ_{\min} . The displacement δ_k of node k of the truss is compared with δ_{\max} and δ_{\min} . σ_{\max} and σ_{\min} are the maximum allowable normal stress limit for both tension and compression. δ_{\max} and δ_{\min} are the maximum and minimum permissible nodal displacement value.

Fig. 1 illustrates the example of two-bar planar truss to introduce the notation mentioned above. The number of design variables for sizing and shape are both 2 in this example. Moreover, 3 nodes are included. x_k , y_k , and z_k are the coordinates of node k in the x , y , and z directions. R_k^x , R_k^y , and R_k^z are the x , y , and z components of reaction force applied to node k .

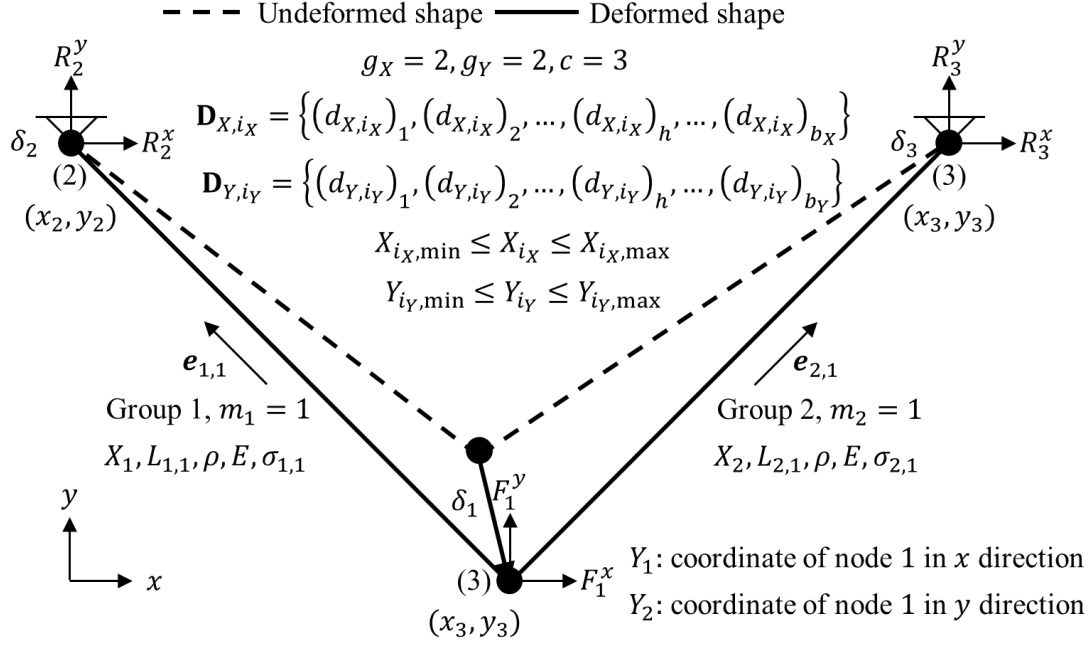


Fig. 1 Two-bar planar truss for sizing and shape optimization of truss structures

2.2 IMCTS formulation for discrete sizing optimization of truss structures

An RL-based algorithm using IMCTS formulation was first proposed by Ko et al. (2024) to solve sizing optimization of truss structures with discrete variable. IMCTS formulation proposed the novel concept including update process and accelerating technique for discrete variable, the best reward, and terminal condition. These concepts are used in MVSMCTS formulation, which will be further explained in the next section.

2.2.1 Update process for discrete sizing variable and the best reward

The four main components of an MDP for discrete sizing optimization of truss structures were developed by Ko et al. (2024). A state is represented as a set of numerical data of nodes and members. Action is defined as determining the cross-sectional area of each member from a list of discrete values. The environment deterministically leads to a unique next state after executing action from one state. The reward is assigned to the terminal state, which is computed as follows:

$$r_T = (\alpha/W_T)^2 \quad (3)$$

where r_T is the reward for terminal state T , which is a dimensionless quantity; α is the minimum weight; and W_T is the weight of the truss for terminal state.

A search tree is constructed in each round for IMCTS formulation. MCTS originates from the root node denoted as the initial state of the search tree. The four strategic steps of MCTS are repeated until some predefined computational budget is reached (Browne et al. 2012). In the selection step, the upper confidence bound (UCB) for IMCTS

formulation is defined as follows:

$$U_I = V_I + C \sqrt{\frac{\ln N}{n_I}} \quad (4)$$

where I is the index of the node; U_I , V_I , and n_I are the UCB, the estimate of state value, and the number of times the node I has been visited, respectively; N is the total number of simulations executed from the parent node; and C is the constant parameter that adjusts the selection strategy. For IMCTS formulation, the best reward is used in the backpropagation step, which is calculated as follows:

$$V_I \leftarrow \max(V_I, G_{\tau_N}) \quad (5)$$

where G_{τ_N} is the simulation result of the path τ_N from the root node or the parent node. Moreover, n_I increases by 1 for all nodes along the path.

MCTS starts from the root node or the parent node and continues executing the four steps. After reaching maximum number of iterations for that node, a child node with the largest estimate of state value is selected. This process is called policy improvement. Then, the selected node is regarded as the parent node for the next policy improvement. After many policy improvements, terminal node is determined. Then, the final state \bar{s}^p , the final weight \bar{W}^p , and the final sizing vector \bar{X}^p in round p are determined.

Update process shown in Fig. 2 indicates that \bar{X}^p is used as the sizing vector \mathbf{X}_0^{p+1} for initial state s_0^{p+1} in round $(p + 1)$. The starting point of the search for sizing variable is the maximum value. Therefore, all sizing variables for initial state s_0^1 in round 1 is equal to the largest element in a list \mathbf{D}_{X,i_X} , i.e., d_{X,b_X} . In order to describe the action and action space of initial and intermediate state for discrete sizing variable, a list \mathbf{D}_{X,i_X}^p belonging to \mathbf{D}_{X,i_X} in round p is defined as follows:

$$\mathbf{D}_{X,i_X}^p = \left\{ (d_{X,i_X}^p)_1, \dots, (d_{X,i_X}^p)_h, \dots, (d_{X,i_X}^p)_\mu, \dots, (d_{X,i_X}^p)_{\beta_X^p} \right\} \quad (6)$$

where $(d_{X,i_X}^p)_h$ is the element in a list \mathbf{D}_{X,i_X}^p ; $(d_{X,i_X}^p)_\mu$ is the median of a list \mathbf{D}_{X,i_X}^p and equal to $(X_{i_X}^p)_0$; and β_X^p is the number of elements in a list \mathbf{D}_{X,i_X}^p .

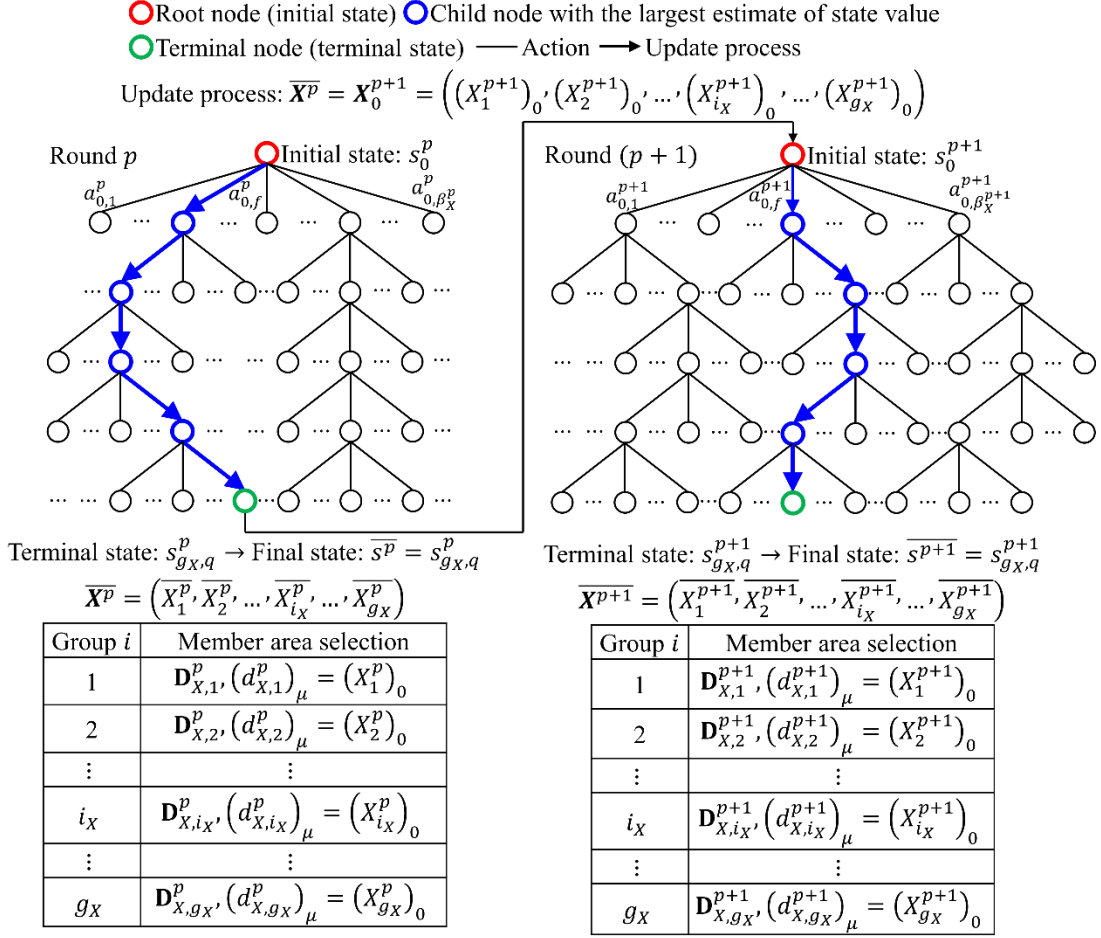


Fig. 2 Update process for discrete sizing variable

2.2.2 Accelerating technique for discrete sizing variable

Accelerating technique for discrete sizing variable is developed by decreasing the width of search tree during the update process. The width of search tree is based on β_X^p . Three types of accelerating techniques are considered in the IMCTS formulation: (1) geometric decay, (2) linear decrease, and (3) step reduction. Geometric decay is the most efficient approach, which is computed as follows:

$$\beta_X^1 = \begin{cases} b_X & \text{if } b_X \text{ is odd number} \\ b_X + 1 & \text{if } b_X \text{ is even number} \end{cases} \quad (7a)$$

$$\varphi_X^p = \beta_X^1 \times \gamma_X^{\lfloor \frac{p-1}{\epsilon_X} \rfloor} \quad (7b)$$

$$\phi_X^p = \lfloor \varphi_X^p \rfloor \quad (7c)$$

$$\omega_X^p = \begin{cases} \phi_X^p & \text{if } \phi_X^p \text{ is odd number} \\ \phi_X^p + 1 & \text{if } \phi_X^p \text{ is even number} \end{cases} \quad (7d)$$

$$\beta_X^p = \max(3, \omega_X^p) \quad (p > 1) \quad (7e)$$

where γ_X and ϵ_X are constant parameters to adjust β_X^p , which are set to 0.5 and 3; $\lfloor \frac{p-1}{\epsilon_X} \rfloor$

is the least integer greater than or equal to $\frac{p-1}{\epsilon_X}$; $\lfloor \varphi_X^p \rfloor$ is the greatest integer less than or equal to φ_X^p ; and $\max(3, \omega_X^p)$ is the maximum value between 3 and ω_X^p .

2.2.3 Terminal condition

For terminal condition, improvement factor η and counter θ are used to ensure the convergence of the algorithm. The improvement factor is defined as follows:

$$\eta = |(\overline{W}^p - \min(\mathbf{S})) / \min(\mathbf{S}) \times 100\%| \quad (8)$$

where \mathbf{S} is a list to store the final weight \overline{W}^p ; and $\min(\mathbf{S})$ is the smallest element in a list \mathbf{S} . Before executing an algorithm, \overline{W}^0 is in a list \mathbf{S} , and θ is set to 0. \overline{W}^0 is the maximum weight. At the end of the round, the improvement factor is calculated, and then \overline{W}^p is inserted in a list \mathbf{S} . When $\eta < \eta_{\min}$, θ increases by 1. When $\theta \geq \theta_{\max}$, the algorithm terminates. η_{\min} and θ_{\max} are the critical value of improvement factor and the maximum number of counters for termination, which are set to 0.01% and 3. At this time, $\min(\mathbf{S})$ is the optimal solution of the optimization problem.

3 MVSMCTS formulation for mixed variable structural optimization- Take sizing and shape optimization of truss structures as an example

Update process for discrete variable outlined in the previous section can be easily applied for continuous variable. Then, update process for discrete shape variable is briefly mentioned, which is similar to that for discrete sizing variable. Finally, MVSMCTS formulation considering different types of variables with mixed continuous-discrete system is described. Sizing and shape variable are considered in this study.

3.1 MVSMCTS formulation for continuous sizing and shape variable

3.1.1 Update process

For update process, it is desirable to handle the sizing and shape variable in the same computational framework. It means that $\overline{\mathbf{X}}^p$ and $\overline{\mathbf{Y}}^p$ in round p is utilized as the sizing vector \mathbf{X}_0^{p+1} and the shape vector \mathbf{Y}_0^{p+1} for initial state s_0^{p+1} in round $(p+1)$. The starting point of the search for sizing variable is the maximum value as described in Sect. 2.2.1. However, the starting point of a path for shape variable is the center of entire search region. Therefore, \mathbf{X}_0^1 and \mathbf{Y}_0^1 is expressed as follows:

$$\mathbf{X}_0^1 = ((X_1^1)_0, \dots, (X_{i_X}^1)_0, \dots, (X_{g_X}^1)_0) = (X_{1,\max}, \dots, X_{i_X,\max}, \dots, X_{g_X,\max}) \quad (9)$$

$$\mathbf{Y}_0^1 = \left((Y_1^1)_0, \dots, (Y_{i_Y}^1)_0, \dots, (Y_{g_Y}^1)_0 \right) = (Y_{1,\text{med}}, \dots, Y_{i_Y,\text{med}}, \dots, Y_{g_Y,\text{med}}) \quad (10a)$$

$$Y_{i_Y,\text{med}} = 0.5 \times (Y_{i_Y,\text{min}} + Y_{i_Y,\text{max}}) \quad (10b)$$

The search region in each round is determined from the design variable for initial state. Therefore, the left-hand side and right-hand side of search region for sizing and shape variable in round p are defined as follows:

$$X_{i_X,\text{min}}^p = (X_{i_X}^p)_0 - A_X \times \xi_{X,i_X}^p \quad (11a)$$

$$X_{i_X,\text{max}}^p = (X_{i_X}^p)_0 + (1 - A_X) \times \xi_{X,i_X}^p \quad (11b)$$

$$Y_{i_Y,\text{min}}^p = (Y_{i_Y}^p)_0 - A_Y \times \xi_{Y,i_Y}^p \quad (12a)$$

$$Y_{i_Y,\text{max}}^p = (Y_{i_Y}^p)_0 + (1 - A_Y) \times \xi_{Y,i_Y}^p \quad (12b)$$

where $X_{i_X,\text{min}}^p$ and $Y_{i_Y,\text{min}}^p$ are the left-hand side of search region; $X_{i_X,\text{max}}^p$ and $Y_{i_Y,\text{max}}^p$ are the right-hand side of search region; ξ_{X,i_X}^p and ξ_{Y,i_Y}^p are the range of search region, which decreases when more round is reached; and A_X and A_Y are constant parameters to determine the position in search region for expansion. The design variable for initial state is set to the left-hand side, the center, and the right-hand side of search region when A_X and A_Y are all equal to 0, 0.5, and 1. The schematic diagram for expansion of search region is depicted in Fig. 3.

In order to adopt MCTS in continuous space, uniform meshes are generated automatically in search region in each round. Therefore, lists \mathbf{Y}_{X,i_X}^p and \mathbf{Y}_{Y,i_Y}^p for continuous sizing and shape variable in round p are as follows:

$$\mathbf{Y}_{X,i_X}^p = \left\{ (v_{X,i_X}^p)_1, (v_{X,i_X}^p)_2, \dots, (v_{X,i_X}^p)_h, \dots, (v_{X,i_X}^p)_{\kappa_X^p} \right\} \quad (13)$$

$$\mathbf{Y}_{Y,i_Y}^p = \left\{ (v_{Y,i_Y}^p)_1, (v_{Y,i_Y}^p)_2, \dots, (v_{Y,i_Y}^p)_h, \dots, (v_{Y,i_Y}^p)_{\kappa_Y^p} \right\} \quad (14)$$

where $(v_{X,i_X}^p)_h$ and $(v_{Y,i_Y}^p)_h$ are the elements in lists \mathbf{Y}_{X,i_X}^p and \mathbf{Y}_{Y,i_Y}^p ; and κ_X^p and κ_Y^p are

the number of elements in lists \mathbf{Y}_{X,i_X}^p and \mathbf{Y}_{Y,i_Y}^p . It is worth noting that $(v_{X,i_X}^p)_1$, $(v_{X,i_X}^p)_{\kappa_X^p}$,

$(v_{Y,i_Y}^p)_1$, and $(v_{Y,i_Y}^p)_{\kappa_Y^p}$ are $X_{i_X,\text{min}}^p$, $X_{i_X,\text{max}}^p$, $Y_{i_Y,\text{min}}^p$, and $Y_{i_Y,\text{max}}^p$, respectively. For

continuous sizing and shape variable, action $a_{l_X,f}^p$ ($l_X = 0, 1, \dots, g_X - 1$) and $a_{l_Y,f}^p$ ($l_Y = 0, 1, \dots, g_Y - 1$) for initial and intermediate state is expressed as follows:

$$a_{l_X,f}^p: M_{X,i_X}^p: 1 \rightarrow 0 \text{ and } X_{i_X}^p: (X_{i_X}^p)_0 \rightarrow (v_{X,i_X}^p)_h \quad (i_X = l_X + 1, f = h) \quad (15)$$

$$a_{i_Y, f}^p: M_{Y, i_Y}^p: 1 \rightarrow 0 \text{ and } Y_{i_Y}^p: (Y_{i_Y}^p)_0 \rightarrow (v_{Y, i_Y}^p)_h \text{ (} i_Y = l_Y + 1, f = h \text{)} \quad (16)$$

where M_{X, i_X}^p and M_{Y, i_Y}^p are used to confirm when the cross-sectional area of group i_X and the nodal coordinate of node i_Y are determined in round p ; $X_{i_X}^p$ is the cross-sectional area; and $Y_{i_Y}^p$ is the nodal coordinate. $M_{X, i_X}^p = 1$ and $M_{Y, i_Y}^p = 1$ when X_{i_X} and Y_{i_Y} are not determined, and $M_{X, i_X}^p = 0$ and $M_{Y, i_Y}^p = 0$ otherwise. The action spaces of s_0^p , $s_{l_X, q}^p$, and $s_{l_Y, q}^p$ are as follows:

$$\mathcal{A}(s_0^p) = \{a_{0,1}^p, a_{0,2}^p, \dots, a_{0,f}^p, \dots, a_{0, \kappa_X^p}^p\} \quad (17a)$$

$$\mathcal{A}(s_{l_X, q}^p) = \{a_{l_X,1}^p, a_{l_X,2}^p, \dots, a_{l_X, f}^p, \dots, a_{l_X, \kappa_X^p}^p\} \quad (17b)$$

$$\mathcal{A}(s_0^p) = \{a_{0,1}^p, a_{0,2}^p, \dots, a_{0,f}^p, \dots, a_{0, \kappa_Y^p}^p\} \quad (18a)$$

$$\mathcal{A}(s_{l_Y, q}^p) = \{a_{l_Y,1}^p, a_{l_Y,2}^p, \dots, a_{l_Y, f}^p, \dots, a_{l_Y, \kappa_Y^p}^p\} \quad (18b)$$

The schematic diagram of update process for continuous sizing and shape variable is depicted in Fig. 3.

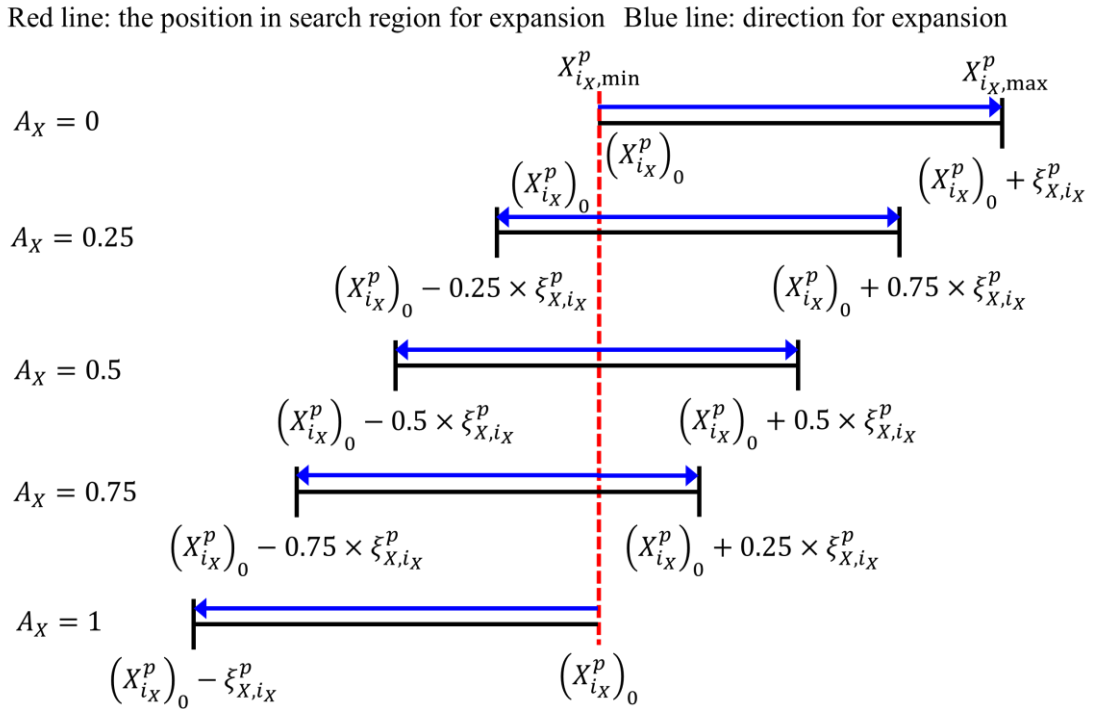


Fig. 3 Schematic diagram for expansion of search region in continuous space

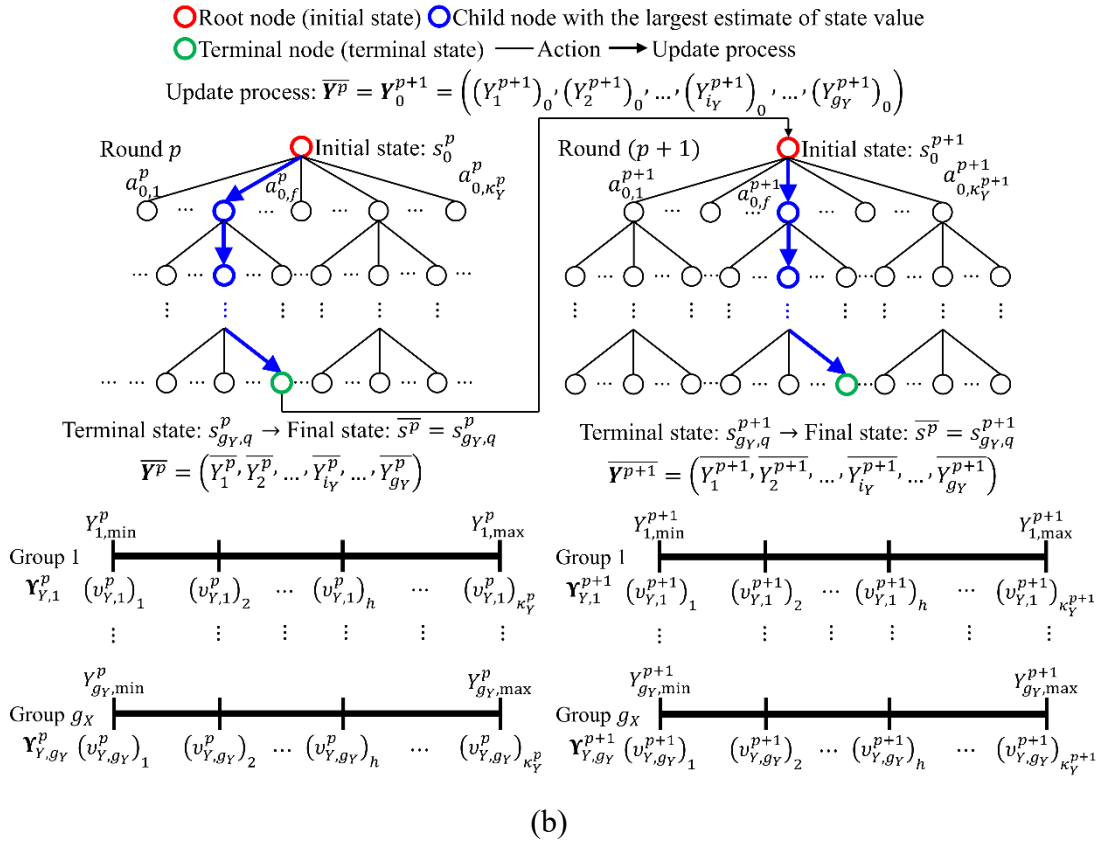
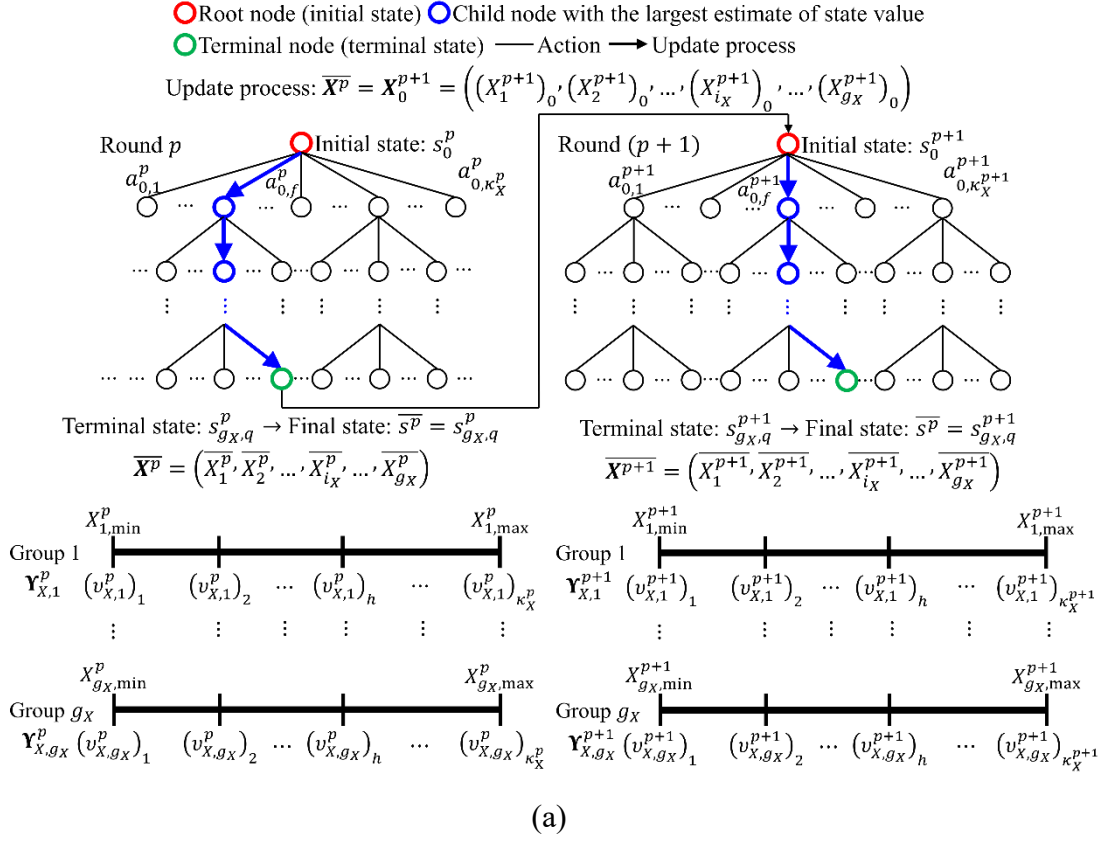


Fig. 4 Schematic diagram of update process for continuous (a) sizing and (b) shape variable

3.1.2 Accelerating technique

The range of search region and the width of search tree are not changed during update process when accelerating technique is not considered, as shown in Fig. 5(a). It means that ξ_{X,i_X}^p , κ_X^p , ξ_{Y,i_Y}^p , and κ_Y^p are constants in each round, which is formulated as follows:

$$\xi_{X,i_X}^1 = \xi_{X,i_X}^2 = \dots = \xi_{X,i_X}^p = \dots = X_{i_X,\max} - X_{i_X,\min} \quad (19a)$$

$$\kappa_X^1 = \kappa_X^2 = \dots = \kappa_X^p = \dots = g_X \quad (19b)$$

$$\xi_{Y,i_Y}^1 = \xi_{Y,i_Y}^2 = \dots = \xi_{Y,i_Y}^p = \dots = Y_{i_Y,\max} - Y_{i_Y,\min} \quad (20a)$$

$$\kappa_Y^1 = \kappa_Y^2 = \dots = \kappa_Y^p = \dots = g_Y \quad (20b)$$

From Eqs. 19 and 20, it is shown that ξ_{X,i_X}^p and ξ_{Y,i_Y}^p are equal to the difference between the lower and the upper limit for sizing and shape. Moreover, κ_X^p and κ_Y^p are equal to the number of design variables for sizing and shape.

Accelerating technique is developed by decreasing the range of search region and the width of search tree as the update process proceeds, as shown in Fig. 5(b). Three types of accelerating techniques mentioned in Sect. 2.2.2 are used to determine the range of search region. For geometric decay, ξ_{X,i_X}^p and ξ_{Y,i_Y}^p are computed as follows:

$$\xi_{X,i_X}^1 = X_{i_X,\max} - X_{i_X,\min} \quad (21a)$$

$$\xi_{X,i_X}^p = \xi_{X,i_X}^1 \times \lambda_{X,geo}^{\left\lfloor \frac{p-1}{\varpi_{X,geo}} \right\rfloor} \quad (21b)$$

$$\xi_{Y,i_Y}^1 = Y_{i_Y,\max} - Y_{i_Y,\min} \quad (22a)$$

$$\xi_{Y,i_Y}^p = \xi_{Y,i_Y}^1 \times \lambda_{Y,geo}^{\left\lfloor \frac{p-1}{\varpi_{Y,geo}} \right\rfloor} \quad (22b)$$

where $\lambda_{X,geo}$, $\varpi_{X,geo}$, $\lambda_{Y,geo}$, and $\varpi_{Y,geo}$ are constant parameters for geometric decay

to adjust ξ_{X,i_X}^p and ξ_{Y,i_Y}^p in each round; and $\left\lfloor \frac{p-1}{\varpi_{X,geo}} \right\rfloor$ and $\left\lfloor \frac{p-1}{\varpi_{Y,geo}} \right\rfloor$ are the least integers

greater than or equal to $\frac{p-1}{\varpi_{X,geo}}$ and $\frac{p-1}{\varpi_{Y,geo}}$. In this study, $\lambda_{X,geo}$ and $\lambda_{Y,geo}$ are all set to

0.5, and $\varpi_{X,geo}$ and $\varpi_{Y,geo}$ are set to 3 and 5 in this study. As seen from Eqs. 21a and

22a, ξ_{X,i_X}^1 and ξ_{Y,i_Y}^1 are equal to the difference between the minimum and the maximum

allowable value for sizing and shape. In order to reduce the execution time, ξ_{X,i_X}^p and

ξ_{Y,i_Y}^p are decreasing geometrically when reaching more rounds. Hence, Eqs. 21b and

22b are utilized to satisfy this requirement.

For linear decrease, ξ_{X,i_X}^p and ξ_{Y,i_Y}^p are calculated as follows:

$$\xi_{X,i_X}^1 = X_{i_X,\max} - X_{i_X,\min} \quad (23a)$$

$$\xi_{X,i_X}^p = \xi_{X,i_X}^1 - \lambda_{X,lin}(p-1) \quad (23b)$$

$$\xi_{X,i_X}^p = \max(\xi_{X,i_X}^{lin}, \xi_{X,i_X}^p) \quad (p > 1) \quad (23c)$$

$$\xi_{X,i_X}^{lin} = \lambda_{X,lin} \times \xi_{X,i_X}^1 \quad (23d)$$

$$\xi_{Y,i_Y}^1 = Y_{i_Y,max} - Y_{i_Y,min} \quad (24a)$$

$$\xi_{Y,i_Y}^p = \xi_{Y,i_Y}^1 - \lambda_{Y,lin}(p - 1) \quad (24b)$$

$$\xi_{Y,i_Y}^p = \max(\xi_{Y,i_Y}^{lin}, \xi_{Y,i_Y}^p) \quad (p > 1) \quad (24c)$$

$$\xi_{Y,i_Y}^{lin} = \lambda_{Y,lin} \times \xi_{Y,i_Y}^1 \quad (24d)$$

where $\lambda_{X,lin}$ and $\lambda_{Y,lin}$ are constant parameters for linear decrease to adjust ξ_{X,i_X}^p and ξ_{Y,i_Y}^p in each round, which are all set to 0.05 in this study; and ξ_{X,i_X}^{lin} and ξ_{Y,i_Y}^{lin} are the critical values of linear decrease for ξ_{X,i_X}^p and ξ_{Y,i_Y}^p , respectively. From Eqs. 23b and 24b, it is seen that ξ_{X,i_X}^p and ξ_{Y,i_Y}^p are decreasing linearly when more round is reached. Eqs. 23c and 24c are employed to ensure that ξ_{X,i_X}^p and ξ_{Y,i_Y}^p are all positive real numbers during update process.

For step reduction, ξ_{X,i_X}^p and ξ_{Y,i_Y}^p can be expressed as follows:

$$\xi_{X,i_X}^1 = X_{i_X,max} - X_{i_X,min} \quad (25a)$$

$$\xi_{X,i_X}^p = \xi_{X,i_X}^1 - \lambda_{X,red} \left\lfloor \frac{p-1}{\varpi_{X,red}} \right\rfloor \quad (25b)$$

$$\xi_{X,i_X}^p = \max(\xi_{X,i_X}^{red}, \xi_{X,i_X}^p) \quad (p > 1) \quad (25c)$$

$$\xi_{X,i_X}^{red} = \lambda_{X,red} \times \xi_{X,i_X}^1 \quad (25d)$$

$$\xi_{Y,i_Y}^1 = Y_{i_Y,max} - Y_{i_Y,min} \quad (26a)$$

$$\xi_{Y,i_Y}^p = \xi_{Y,i_Y}^1 - \lambda_{Y,red} \left\lfloor \frac{p-1}{\varpi_{Y,red}} \right\rfloor \quad (26b)$$

$$\xi_{Y,i_Y}^p = \max(\xi_{Y,i_Y}^{red}, \xi_{Y,i_Y}^p) \quad (p > 1) \quad (26c)$$

$$\xi_{Y,i_Y}^{red} = \lambda_{Y,red} \times \xi_{Y,i_Y}^1 \quad (26d)$$

where $\lambda_{X,red}$, $\varpi_{X,red}$, $\lambda_{Y,red}$, $\varpi_{Y,red}$ are constant parameters for step reduction to adjust ξ_{X,i_X}^p and ξ_{Y,i_Y}^p in each round, which are set to 0.05, 3, 0.05, and 5 in this study; and ξ_{X,i_X}^{red} and ξ_{Y,i_Y}^{red} are the critical values of step reduction for ξ_{X,i_X}^p and ξ_{Y,i_Y}^p , respectively. In Eqs. 25b and 26b, it is shown that ξ_{X,i_X}^p and ξ_{Y,i_Y}^p are the step function of p .

The width of search tree is based on the number of meshes automatically generated in continuous space. In other words, κ_X^p and κ_Y^p are utilized to determine the width of search tree in each round. There are three types of accelerating techniques to calculate κ_X^p and κ_Y^p , which is similar to that for discrete variable presented in Sect. 2.2.2. For geometric decay, κ_X^p and κ_Y^p are expressed as follows:

$$\kappa_X^1 = g_X \quad (27a)$$

$$\psi_X^p = \kappa_X^1 \times \varrho_{X,geo} \left\lfloor \frac{p-1}{\zeta_{X,geo}} \right\rfloor \quad (27b)$$

$$\kappa_X^p = \max(3, \lfloor \psi_X^p \rfloor) \quad (p > 1) \quad (27c)$$

$$\kappa_Y^1 = g_Y \quad (28a)$$

$$\psi_Y^p = \kappa_Y^1 \times \varrho_{Y,geo} \left\lceil \frac{p-1}{\varsigma_{Y,geo}} \right\rceil \quad (28b)$$

$$\kappa_Y^p = \max(3, \lfloor \psi_Y^p \rfloor) \quad (p > 1) \quad (28c)$$

where $\varrho_{X,geo}$, $\varsigma_{X,geo}$, $\varrho_{Y,geo}$, and $\varsigma_{Y,geo}$ are constant parameters to adjust κ_X^p and κ_Y^p in each round, which are set to 0.5, 3, 0.5, and 5 in this study; $\left\lceil \frac{p-1}{\varsigma_{X,geo}} \right\rceil$ and $\left\lceil \frac{p-1}{\varsigma_{Y,geo}} \right\rceil$ are the least integers greater than or equal to $\frac{p-1}{\varsigma_{X,geo}}$ and $\frac{p-1}{\varsigma_{Y,geo}}$; $\lfloor \psi_X^p \rfloor$ and $\lfloor \psi_Y^p \rfloor$ are the greatest integers less than or equal to ψ_X^p and ψ_Y^p . Eqs. 27a and 28a indicate that κ_X^1 and κ_Y^1 are equal to the number of design variables for sizing and shape. In order to reduce the computation time, κ_X^p and κ_Y^p are decreasing geometrically when more round is reached. Therefore, Eqs. 27b and 28b are employed to fulfill the requirements. It is worth mentioning that κ_X^p and κ_Y^p are unnecessary to be odd number for continuous variable since κ_X^p and κ_Y^p are utilized to determine the number of meshes automatically generated in search region. In Eqs. 27c and 28c, the minimum value of κ_X^p and κ_Y^p needs to be 3 because there are three parts in search region: the left-hand side, the center, and the right-hand side.

For linear decrease, κ_X^p and κ_Y^p are given as follows:

$$\kappa_X^1 = g_X \quad (29a)$$

$$\Gamma_X^p = \kappa_X^1 - \varrho_{X,lin}(p-1) \quad (29b)$$

$$\kappa_X^p = \max(3, \lfloor \Gamma_X^p \rfloor) \quad (p > 1) \quad (29c)$$

$$\kappa_Y^1 = g_Y \quad (30a)$$

$$\Gamma_Y^p = \kappa_Y^1 - \varrho_{Y,lin}(p-1) \quad (30b)$$

$$\kappa_Y^p = \max(3, \lfloor \Gamma_Y^p \rfloor) \quad (p > 1) \quad (30c)$$

where $\varrho_{X,lin}$ and $\varrho_{Y,lin}$ are constant parameters for linear decrease to adjust κ_X^p and κ_Y^p in each round, which are all set to 2 in this study. From Eqs. 29b and 30b, κ_X^p and κ_Y^p are decreasing linearly when reaching more rounds.

For step reduction, κ_X^p and κ_Y^p are expressed as follows:

$$\kappa_X^1 = g_X \quad (31a)$$

$$\Omega_X^p = \kappa_X^1 - \varrho_{X,red} \left\lceil \frac{p-1}{\varsigma_{X,red}} \right\rceil \quad (31b)$$

$$\kappa_X^p = \max(3, \lfloor \Omega_X^p \rfloor) \quad (p > 1) \quad (31c)$$

$$\kappa_Y^1 = g_Y \quad (32a)$$

$$\Omega_Y^p = \kappa_Y^1 - \varrho_{Y,red} \left\lceil \frac{p-1}{\varsigma_{Y,red}} \right\rceil \quad (32b)$$

$$\kappa_Y^p = \max(3, \lfloor \Omega_Y^p \rfloor) \quad (p > 1) \quad (32c)$$

where $Q_{X,red}$, $\varsigma_{X,red}$, $Q_{Y,red}$, and $\varsigma_{Y,red}$ are constant parameters for step reduction to adjust κ_X^p and κ_Y^p in each round, which are set to 2, 3, 2, and 5 in this study. As seen from Eqs. 31b and 32b, κ_X^p and κ_Y^p are the step function of p .

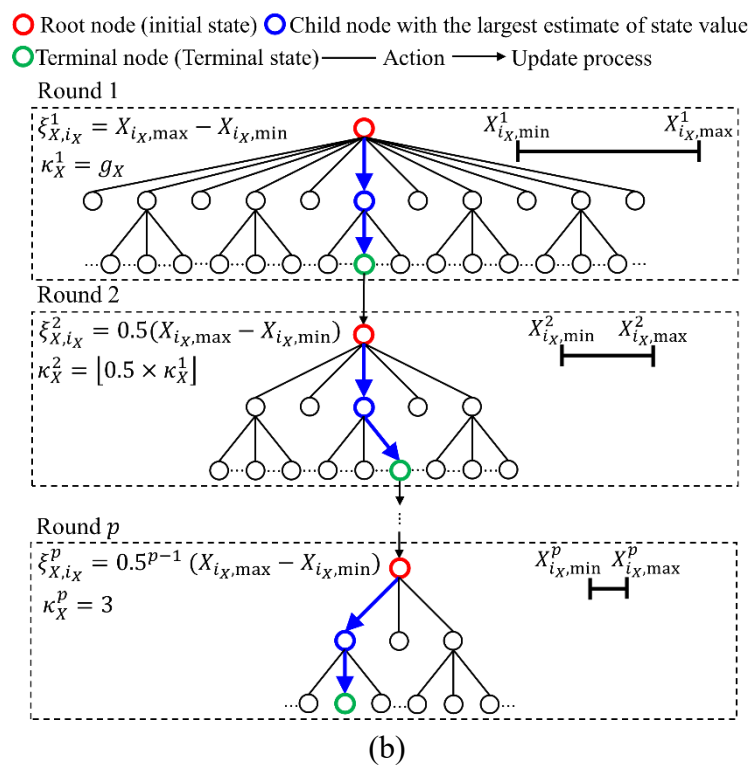
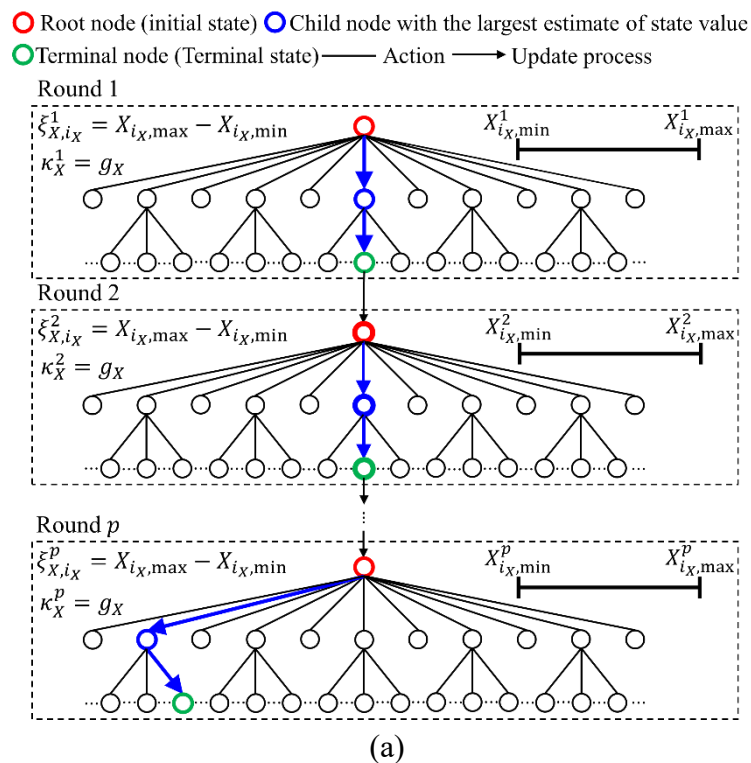


Fig. 5 MVSMCTS formulation for continuous variable (a) without and (b) with accelerating technique (geometric decay)

3.2 MVSMCTS formulation for discrete shape variable

3.2.1 Update process

Update process for discrete shape variable is the same as that for continuous one in Sect. 3.1.1. As mentioned previously, the starting point of the search for shape variable is the center of entire search region. Therefore, \mathbf{Y}_0^1 is described as follows:

$$\mathbf{Y}_0^1 = \left((Y_1^1)_0, \dots, (Y_{i_Y}^1)_0, \dots, (Y_{g_Y}^1)_0 \right) = \left((d_{Y,1})_\mu, \dots, (d_{Y,i_Y})_\mu, \dots, (d_{Y,g_Y})_\mu \right) \quad (33)$$

where $(d_{Y,i_Y})_\mu$ is the median of a list \mathbf{D}_{Y,i_Y} . In order to describe the action and action space of initial and intermediate state for discrete shape variable, a list \mathbf{D}_{Y,i_Y}^p belonging to \mathbf{D}_{Y,i_Y} in round p is defined as follows:

$$\mathbf{D}_{Y,i_Y}^p = \left\{ (d_{Y,i_Y}^p)_1, \dots, (d_{Y,i_Y}^p)_h, \dots, (d_{Y,i_Y}^p)_\mu, \dots, (d_{Y,i_Y}^p)_{\beta_Y^p} \right\} \quad (34)$$

where $(d_{Y,i_Y}^p)_h$ is the element in a list \mathbf{D}_{Y,i_Y}^p ; $(d_{Y,i_Y}^p)_\mu$ is the median of a list \mathbf{D}_{Y,i_Y}^p and equal to $(Y_{i_Y}^p)_0$; and β_Y^p is the number of elements in a list \mathbf{D}_{Y,i_Y}^p .

3.2.2 Accelerating technique

The concept of the accelerating technique for discrete shape variable is the same as that for discrete sizing variable. The width of search tree is based on β_Y^p . Three types of accelerating techniques are considered. For geometric decay, β_Y^p is computed as follows:

$$\beta_Y^1 = \begin{cases} b_Y & \text{if } b_Y \text{ is odd number} \\ b_Y + 1 & \text{if } b_Y \text{ is even number} \end{cases} \quad (35a)$$

$$\varphi_Y^p = \beta_Y^1 \times \gamma_Y^{\left\lfloor \frac{p-1}{\epsilon_Y} \right\rfloor} \quad (35b)$$

$$\phi_Y^p = \lfloor \varphi_Y^p \rfloor \quad (35c)$$

$$\omega_Y^p = \begin{cases} \phi_Y^p & \text{if } \phi_Y^p \text{ is odd number} \\ \phi_Y^p + 1 & \text{if } \phi_Y^p \text{ is even number} \end{cases} \quad (35d)$$

$$\beta_Y^p = \max(3, \omega_Y^p) \quad (p > 1) \quad (35e)$$

where γ_Y and ϵ_Y are constant parameters to adjust β_Y^p , which are set to 0.5 and 3; $\left\lfloor \frac{p-1}{\epsilon_Y} \right\rfloor$

is the least integer greater than or equal to $\frac{p-1}{\epsilon_Y}$; $\lfloor \varphi_Y^p \rfloor$ is the greatest integer less than or

equal to φ_Y^p ; and $\max(3, \omega_Y^p)$ is the maximum value between 3 and ω_Y^p . The formulas of linear decrease and step reduction is the same for discrete sizing variable. The only

difference is that subscript X is changed to Y .

3.3 MVSMCTS formulation for sizing and shape optimization of truss structures

3.3.1 MCTS methodology

For MVSMCTS formulation, the search tree is built in each round to consider sizing and shape variable at the same time. The node denotes the state of the current truss structure. s_0^p , $s_{l_{MVS},q}^p$ ($l_{MVS} = 1, 2, \dots, g_X + g_Y - 1$), and $s_{g_X+g_Y,q}^p$ represent the initial state, the intermediate state, and the final state in round p , respectively. The mathematical expressions of s_0^p , $s_{l_{MVS},q}^p$, and $s_{g_X+g_Y,q}^p$ are as follows:

$$\text{State } s_0^p \quad \begin{aligned} M_{X,1}^p &= M_{X,2}^p = \dots = M_{X,g_X}^p = 1 \\ M_{Y,1}^p &= M_{Y,2}^p = \dots = M_{Y,g_Y}^p = 1 \end{aligned} \quad (36a)$$

$$\begin{aligned} &\text{State } s_{l_{MVS},q}^p \\ (l_{MVS} = 1, 2, \dots, g_Y - 1) \quad &M_{X,1}^p = M_{X,2}^p \dots = M_{X,g_X}^p = 1 \\ &M_{Y,1}^p = M_{Y,2}^p = \dots = M_{Y,i_Y}^p = 0 \\ &M_{Y,i_Y+1}^p = M_{Y,i_Y+2}^p = \dots = M_{Y,g_Y}^p = 1 \quad (i_Y = l_{MVS}) \end{aligned} \quad (36b)$$

$$\begin{aligned} &\text{State } s_{l_{MVS},q}^p \\ (l_{MVS} = g_Y) \quad &M_{X,1}^p = M_{X,2}^p = \dots = M_{X,g_X}^p = 1 \\ &M_{Y,1}^p = M_{Y,2}^p = \dots = M_{Y,g_Y}^p = 0 \end{aligned} \quad (36c)$$

$$\begin{aligned} &\text{State } s_{l_{MVS},q}^p \\ (l_{MVS} = g_Y + 1, \dots, \\ g_X + g_Y - 1) \quad &M_{X,1}^p = M_{X,2}^p = \dots = M_{X,i_X}^p = 0 \\ &M_{X,i_X+1}^p = M_{X,i_X+2}^p = \dots = M_{X,g_X}^p = 1 \\ &M_{Y,1}^p = M_{Y,2}^p = \dots = M_{Y,g_Y}^p = 0 \quad (g_Y + i_X = l_{MVS}) \end{aligned} \quad (36d)$$

$$\text{State } s_{g_X+g_Y,q}^p \quad \begin{aligned} M_{X,1}^p &= M_{X,2}^p = \dots = M_{X,g_X}^p = 0 \\ M_{Y,1}^p &= M_{Y,2}^p = \dots = M_{Y,g_Y}^p = 0 \end{aligned} \quad (36e)$$

where l_{MS} is the layer number for MVSMCTS formulation. The root node represents the initial state s_0^p . Nodes with terminal state $s_{g_X+g_Y,q}^p$ are called terminal nodes. The tree edges indicate the possible actions. Action $a_{l_{MVS},f}^p$ ($l_{MVS} = 0, 1, 2, \dots, g_X + g_Y - 1$) for initial and intermediate state is described as follows:

$$a_{l_{MVS},f}^p: M_{Y,i_Y}^p: 1 \rightarrow 0, Y_{i_Y}^p: (Y_{i_Y}^p)_0 \rightarrow (v_{Y,i_Y}^p)_h \quad (i_Y = l_{MVS} + 1, f = h) \quad (37a)$$

$$a_{l_{MVS},f}^p: M_{Y,i_Y}^p: 1 \rightarrow 0, Y_{i_Y}^p: (Y_{i_Y}^p)_0 \rightarrow (d_{Y,i_Y}^p)_h \quad (i_Y = l_{MVS} + 1, f = h) \quad (37b)$$

$$a_{l_{MVS},f}^p: M_{X,i_X}^p: 1 \rightarrow 0, X_{i_X}^p: (X_{i_X}^p)_0 \rightarrow (v_{X,i_X}^p)_h \quad (i_X = l_{MVS} + 1 - g_Y, f = h) \quad (37c)$$

$$a_{l_{MVS},f}^p: M_{X,i_X}^p: 1 \rightarrow 0, X_{i_X}^p: (X_{i_X}^p)_0 \rightarrow (d_{X,i_X}^p)_h \quad (i_X = l_{MVS} + 1 - g_Y, f = h) \quad (37d)$$

where $X_{i_X}^p$ and $Y_{i_Y}^p$ are the cross-sectional area of the group i_X and the nodal coordinate of the node i_Y for that state. The action spaces of s_0^p and $s_{l_{MVS},q}^p$ are as follows:

$$\mathcal{A}(s_0^p) = \{a_{0,1}^p, \dots, a_{0,f}^p, \dots, a_{0,\kappa_Y}^p\} \quad (38a)$$

$$\mathcal{A}(s_0^p) = \{a_{0,1}^p, \dots, a_{0,f}^p, \dots, a_{0,\beta_Y}^p\} \quad (38b)$$

$$\mathcal{A}(s_{l_{MVS},q}^p) = \{a_{l_{MVS},1}^p, \dots, a_{l_{MVS},f}^p, \dots, a_{l_{MVS},\kappa_Y^p}^p\} \quad (l_{MVS} = 1, \dots, g_Y - 1) \quad (38c)$$

$$\mathcal{A}(s_{l_{MVS},q}^p) = \{a_{l_{MVS},1}^p, \dots, a_{l_{MVS},f}^p, \dots, a_{l_{MVS},\beta_Y^p}^p\} \quad (l_{MVS} = 1, \dots, g_Y - 1) \quad (38d)$$

$$\mathcal{A}(s_{l_{MVS},q}^p) = \{a_{l_{MVS},1}^p, \dots, a_{l_{MVS},f}^p, \dots, a_{l_{MVS},\kappa_X^p}^p\} \quad (l_{MVS} = g_Y, \dots, g_Y + g_X - 1) \quad (38e)$$

$$\mathcal{A}(s_{l_{MVS},q}^p) = \{a_{l_{MVS},1}^p, \dots, a_{l_{MVS},f}^p, \dots, a_{l_{MVS},\beta_X^p}^p\} \quad (l_{MVS} = g_Y, \dots, g_Y + g_X - 1) \quad (38f)$$

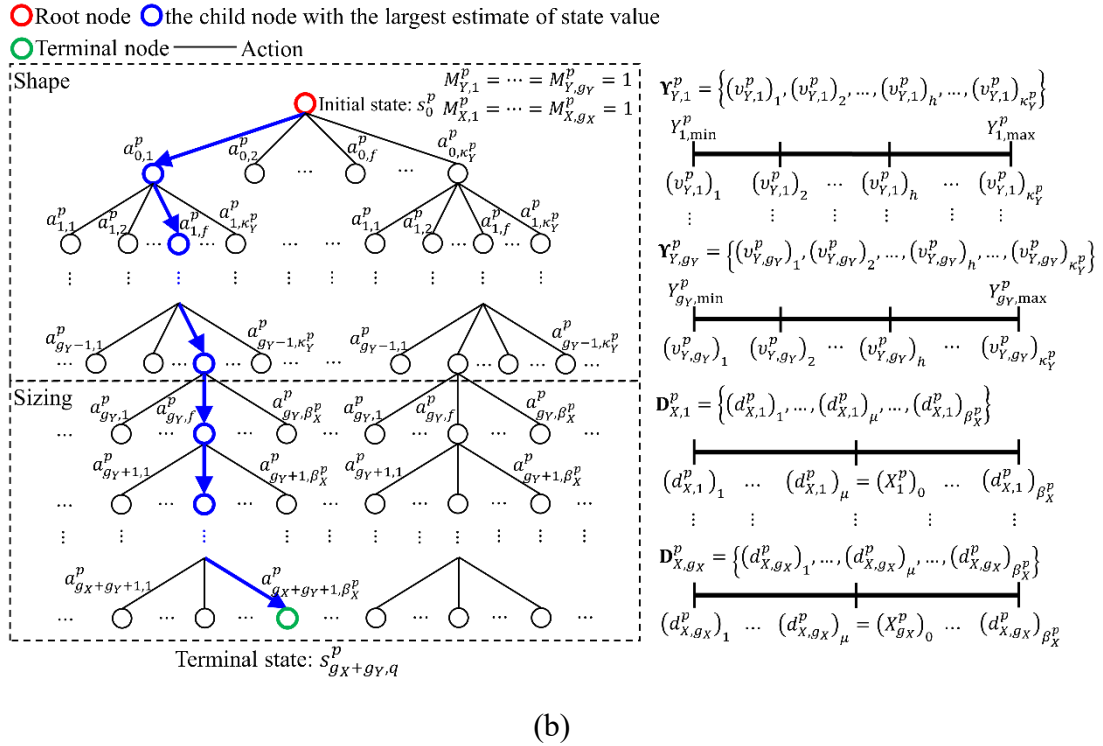
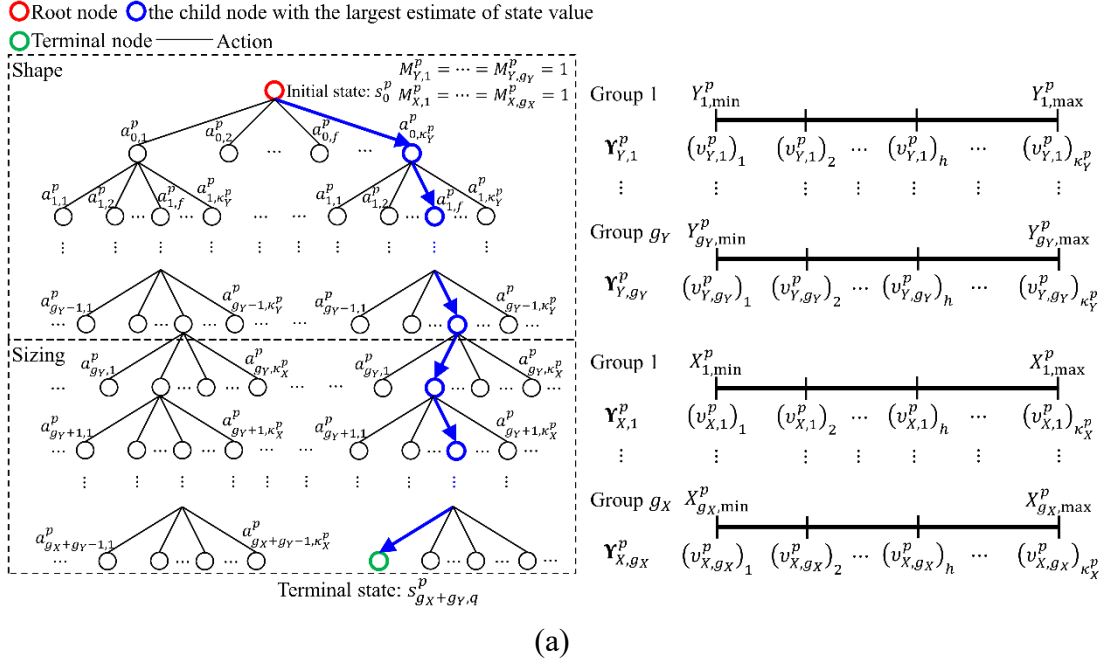


Fig. 6 Search tree used in the MVSMCTS formulation for (a) single continuous-continuous system and (b) mixed continuous-discrete system

MCTS starts constructing the search tree with the root node following the four main steps. The UCB in Eq. 4 and the best reward in Eq. 5 for IMCTS formulation are used in the selection and the backpropagation step for MVMCTS formulation. The search tree considering sizing and shape variable with single and mixed system is shown in Fig. 6.

3.3.2 Policy improvement

Policy improvement for truss optimization on sizing and shape is identical to that for discrete sizing optimization outlined in Sect. 2.2.1. Sizing and shape variable are optimized in one search tree in each round. After many policy improvement steps, terminal node is reached. Then, the final state \bar{s}^p , the final weight \bar{W}^p , the final sizing vector \bar{X}^p , and the final shape vector \bar{Y}^p are all determined. The schematic diagram for policy improvement is shown in Fig. 7.

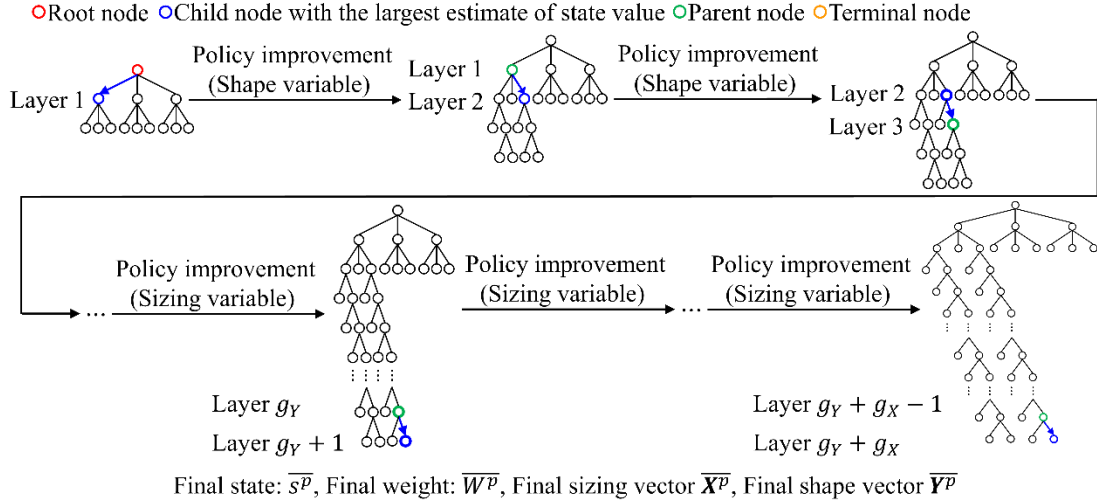


Fig. 7 Policy improvement for MVMCTS formulation

3.3.3 Update process

Update process for MVMCTS formulation shown in Fig. 8 indicates that \bar{X}^p and \bar{Y}^p determined in round p are used as the sizing vector X_0^{p+1} and shape vector Y_0^{p+1} for initial state s_0^{p+1} in round $(p + 1)$. All discrete and continuous sizing variables for initial state in round 1 are equal to $(d_{X,i_X})_{b_X}$ and $X_{i_X,max}$ shown in Sect. 2.2.1 and Eq. 9, respectively. Moreover, all discrete and continuous shape variables for initial state in round 1 are equal to $(d_{Y,i_Y})_{b_Y}$ and $Y_{i_Y,med}$ as in Eqs. 33 and 10, respectively.

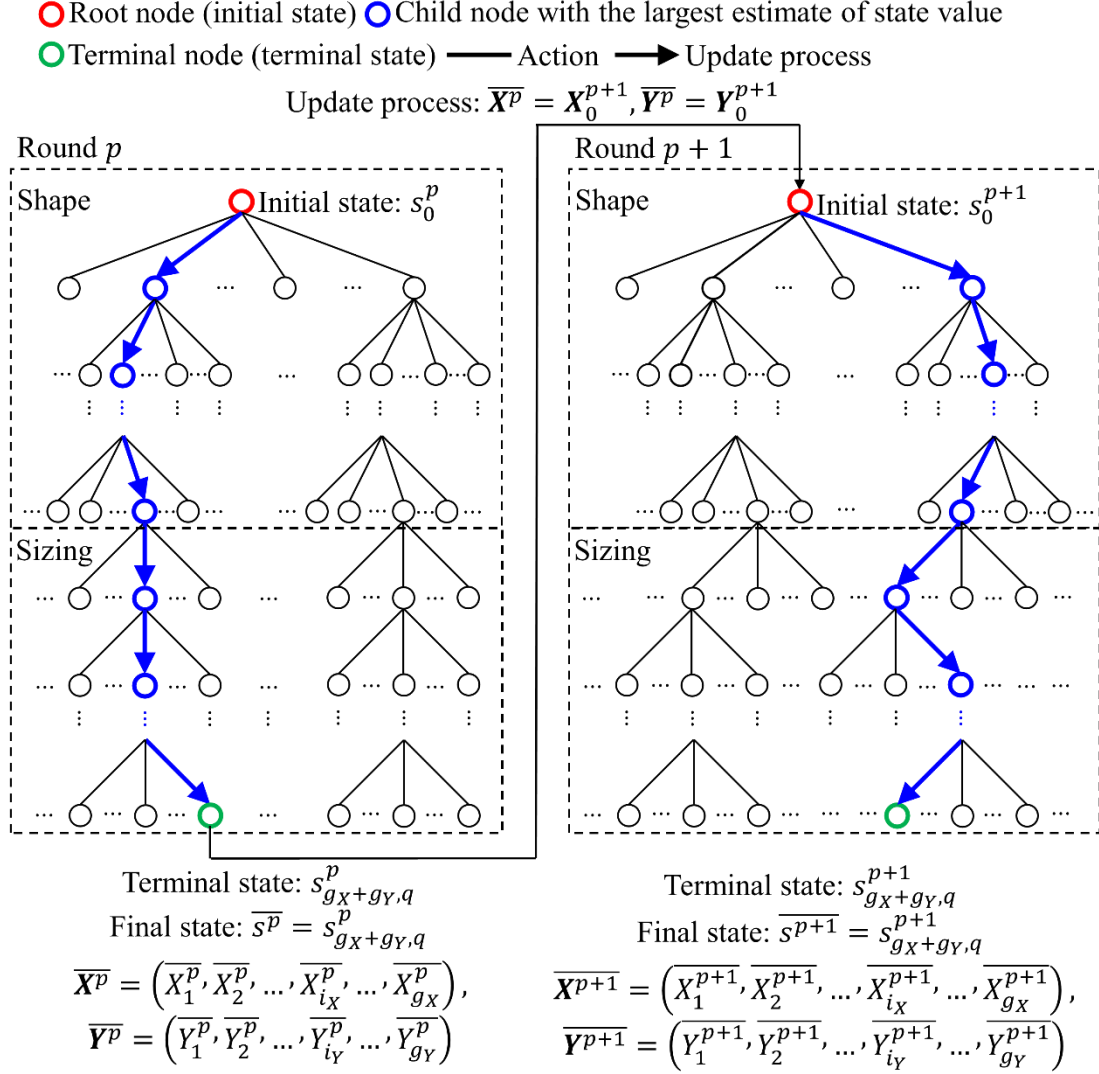


Fig. 8 Update process for MVSMCTS formulation

Accelerating technique for MVSMCTS formulation is based on Eq. 7 for discrete sizing variable, Eqs. 21 and 27 for continuous sizing variable, Eq. 35 for discrete shape variable, and Eqs. 22 and 28 for continuous shape variable. For MVSMCTS formulation, the maximum number of iterations for root node $J_{0,\max}^p$ and parent node $J_{l_{MVS},\max}^p$ for layer l_{MVS} ($l_{MVS} = 1, 2, \dots, g_X + g_Y - 1$) is expressed as follows:

For root node
State s_0^p $J_{0,\max}^p = J_{MVS} \times \lceil \log_{10}(\Psi_X^{g_X} \times \Psi_Y^{g_Y}) \rceil$ (39a)

For parent node
State $s_{l_{MVS},q}^p$ $J_{l_{MVS},\max}^p = J_{MVS} \times \lceil \log_{10}(\Psi_X^{g_X} \times \Psi_Y^{g_Y - l_{MVS}}) \rceil$ (39b)
($l_{MVS} = 1, \dots, g_Y - 1$)

For parent node
State $s_{l_{MVS},q}^p$ $J_{l_{MVS},\max}^p = J_{MVS} \times \lceil \log_{10}(\Psi_X^{g_X}) \rceil$ (39c)
($l_{MVS} = g_Y$)

For parent node
State $s_{l_{MVS},q}^p$ $J_{l_{MVS},\max}^p = J_{MVS} \times \lceil \log_{10}(\Psi_X^{g_X - (l_{MVS} - g_Y)}) \rceil$ (39d)

$$(l_{MVS} = g_Y + 1, \dots, \\ g_X + g_Y - 1)$$

where J_{MVS} is a constant parameter for $J_{0,\max}^p$ and $J_{l_{MVS},\max}^p$ and is set to 3 times the number of design variables in the optimization problem in Sect. 2.1, i.e., $3(g_X + g_Y)$ in this study; Ψ_X are equal to β_X^p and κ_X^p for discrete and continuous sizing variable; and Ψ_Y are equal to β_Y^p and κ_Y^p for discrete and continuous shape variable. The terminal condition for IMCTS formulation outlined in Sect. 2.2.3 is also applicable for MVSMCTS formulation. The pseudo-code and the flowchart of the MVSMCTS formulation for mixed variable structural optimization are illustrated in Figs. 9 and 10.

Algorithm 1: MVSMCTS formulation for sizing and shape optimization of truss structures

- 1 **Initialize** Material density ρ , the modulus of elasticity E , the lists \mathbf{D}_{X,i_X} and \mathbf{D}_{Y,i_Y} , the lower and upper limit $X_{i_X,\min}$, $Y_{i_Y,\min}$, $X_{i_X,\max}$, and $Y_{i_Y,\max}$
- 2 **Initialize** Round number $p = 1$
- 3 **Initialize** Counter $\theta = 0$ and the maximum number of counters for termination $\theta_{\max} = 3$
- 4 **Initialize** Critical value of improvement factor $\eta_{\min} = 0.01$
- 5 **Initialize** List $\mathbf{S} = \{W^0\}$ and the maximum weight \overline{W}^0
- 6 **Initialize** Design variable vector for initial state s_0^1 in round 1 for sizing and shape: \mathbf{X}_0^1 and \mathbf{Y}_0^1
- 7 **While** $\theta \leq \theta_{\max}$ **do**
- 8 Start from a search tree with only root node (initial state s_0^p)
- 9 Define a list $\mathbf{D}_{X,i_X}^p = \left\{ (d_{X,i_X}^p)_1, \dots, (d_{X,i_X}^p)_h, \dots, (d_{X,i_X}^p)_\mu, \dots, (d_{X,i_X}^p)_{\beta_X^p} \right\}$ belonging to \mathbf{D}_{X,i_X} for discrete sizing variable
- 10 Define a list $\mathbf{D}_{Y,i_Y}^p = \left\{ (d_{Y,i_Y}^p)_1, \dots, (d_{Y,i_Y}^p)_h, \dots, (d_{Y,i_Y}^p)_\mu, \dots, (d_{Y,i_Y}^p)_{\beta_Y^p} \right\}$ belonging to \mathbf{D}_{Y,i_Y} for discrete shape variable
- 11 Define a list $\mathbf{Y}_{X,i_X}^p = \left\{ (v_{X,i_X}^p)_1, (v_{X,i_X}^p)_2, \dots, (v_{X,i_X}^p)_h, \dots, (v_{X,i_X}^p)_{\kappa_X^p} \right\}$ for continuous sizing variable, where $(v_{X,i_X}^p)_1 = X_{i_X,\min}^p$ and $(v_{X,i_X}^p)_{\kappa_X^p} = X_{i_X,\max}^p$
- 12 Define a list $\mathbf{Y}_{Y,i_Y}^p = \left\{ (v_{Y,i_Y}^p)_1, (v_{Y,i_Y}^p)_2, \dots, (v_{Y,i_Y}^p)_h, \dots, (v_{Y,i_Y}^p)_{\kappa_Y^p} \right\}$ for continuous shape variable, where $(v_{Y,i_Y}^p)_1 = Y_{i_Y,\min}^p$ and $(v_{Y,i_Y}^p)_{\kappa_Y^p} = Y_{i_Y,\max}^p$
- 13 **While** Terminal node is reached **do**
- 14 **if** Not all shape variable are optimized **then**
- 15 **While** Maximum number of iterations is reached **do**
- 16 Repeat the four strategic steps of MCTS from the root node or the parent node
- 17 Policy improvement (shape variable): select a child node with the largest estimate of state value
- 18 This child node is regarded as the parent node
- 19 **if** Not all sizing variable are optimized **then**
- 20 **While** Maximum number of iterations is reached **do**
- 21 Repeat the four strategic steps of MCTS from the parent node
- 22 Policy improvement (sizing variable): select a child node with the largest estimate of state value
- 23 This child node is regarded as the parent node
- 24 The final state \overline{s}^p is determined, which is the state of the terminal node
- 25 Sizing and shape vector $\overline{\mathbf{X}}^p$ and $\overline{\mathbf{Y}}^p$ are all determined
- 26 The final weight \overline{W}^p is determined
- 27 Calculate improvement factor $\eta = |(\overline{W}^p - \min(\mathbf{S})) / \min(\mathbf{S}) \times 100\%|$
- 28 **if** $\eta \leq \eta_{\min}$ **then**
- 29 $\theta \leftarrow \theta + 1$
- 30 \overline{W}^p is inserted in a list \mathbf{S}
- 31 Update process: $\mathbf{X}_0^{p+1} = \overline{\mathbf{X}}^p$ and $\mathbf{Y}_0^{p+1} = \overline{\mathbf{Y}}^p$
- 32 $p \leftarrow p + 1$
- 33 $\min(\mathbf{S})$ is the optimal solution of the sizing-shape truss optimization problems in Sect. 2.1

Fig. 9 Pseudo-code for the MVSMCTS formulation

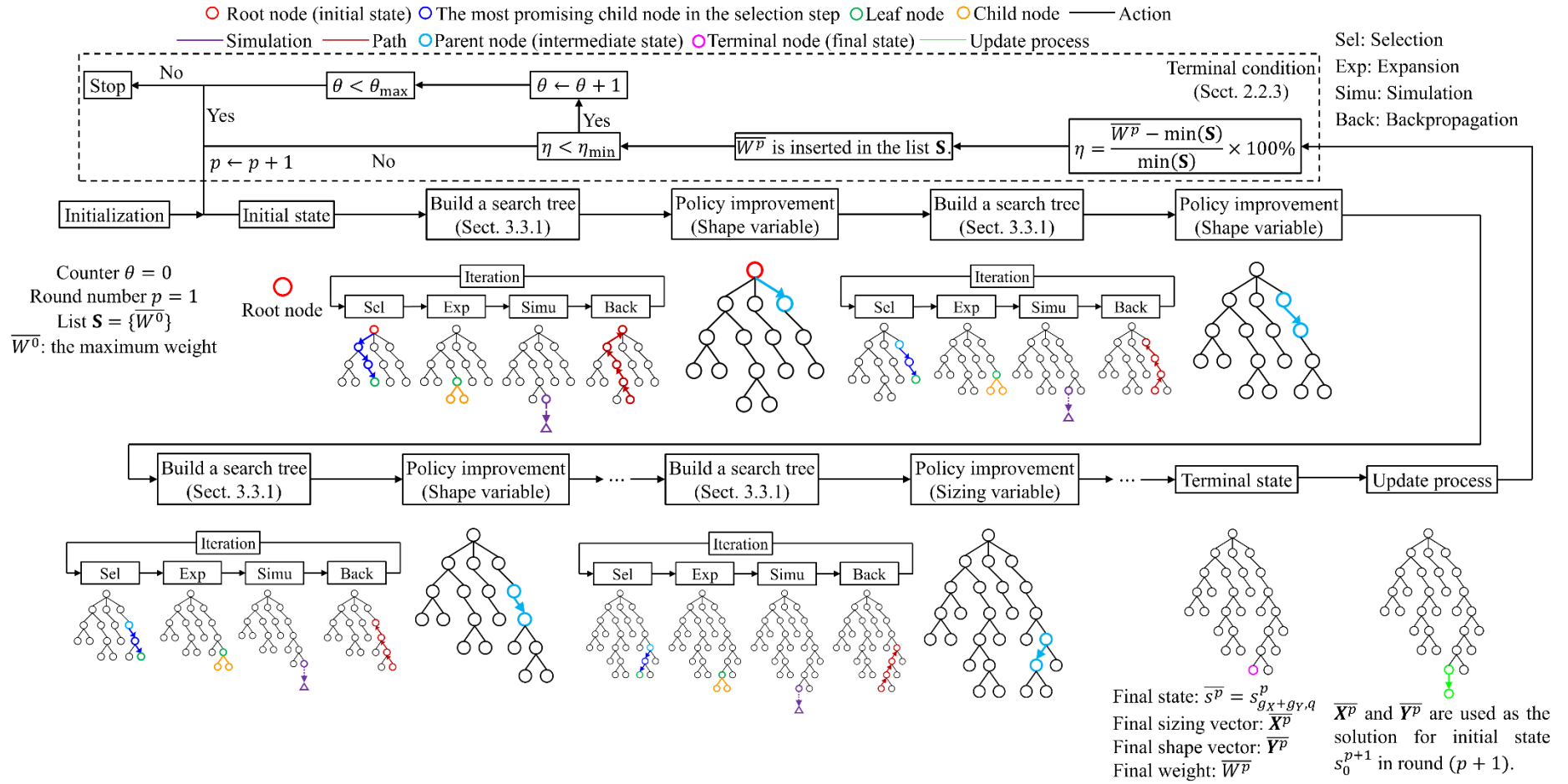


Fig. 10 Flowchart of the MVSMCTS formulation

3.4 Comparisons of IMCTS and MVSMCTS formulation

Table 1 lists the characteristics of IMCTS and MVSMCTS formulation. IMCTS and MVSMCTS formulation are applicable to single type of variable with discrete system and variable types of variables with single and mixed system. Moreover, it is seen that MDP framework, four steps of MCTS, UCB, the best reward, policy improvement, update process and accelerating technique for discrete variable and terminal condition proposed in IMCTS formulation can also be used in MVSMCTS formulation.

Table 1 Comparisons of the IMCTS and MVSMCTS formulation

	IMCTS formulation (Ko et al. 2024)	MVSMCTS formulation
Type of optimization problem	Single type of variable with discrete system	Various types of variables with single and mixed continuous-discrete system
Example	Discrete sizing optimization of truss structure	Truss optimization on sizing and shape
Markov decision process		
State	a set of numerical data of nodes and members	a set of numerical data of nodes and members
Action	determine discrete sizing variable	1. determine discrete and continuous sizing variable 2. determine discrete and continuous shape variable
State transition	deterministic	deterministic
Reward function	$r_T = (\alpha/W_T)^2$ (terminal state)	$r_T = (\alpha/W_T)^2$ (terminal state)
Monte Carlo tree search		
How to build a search tree	the four strategic steps of MCTS	the four strategic steps of MCTS
Selection step	UCB: $U_i = V_i + C \sqrt{\frac{\ln N}{n_i}}$	UCB: $U_i = V_i + C \sqrt{\frac{\ln N}{n_i}}$
Backpropagation step	the best reward: $V_i \leftarrow \max(V_i, G_{\tau_N})$	the best reward: $V_i \leftarrow \max(V_i, G_{\tau_N})$
Policy improvement	Start from root node and conduct policy improvement. After many policy improvement steps, terminal node is reached.	Start from root node and conduct policy improvement. After many policy improvement steps, terminal node is reached.
Algorithm		
Update process	for discrete variable	for discrete and continuous variable ■ continuous: generate uniform meshes automatically in search region ■ multiple root nodes
Search tree	multiple root nodes	■ consider various types of variables in only one search tree ■ for discrete variable ● decrease the width of search tree
Accelerating technique	for discrete variable ● decrease the width of search tree ● reduce maximum number of iterations	● reduce maximum number of iterations ■ for continuous variable ● decrease the width of search tree based on the number of meshes ● decrease the range of search region ● reduce maximum number of iterations
Terminal condition	Improvement factor η and counter θ are defined. When $\eta < \eta_{\min}$, θ is set to $\theta + 1$. If $\theta < \theta_{\max}$, the algorithm terminates.	Improvement factor η and counter θ are defined. When $\eta < \eta_{\min}$, θ is set to $\theta + 1$. If $\theta < \theta_{\max}$, the algorithm terminates.

4 Numerical experiments

The ability of the proposed MVSMCTS formulation is assessed by three weight minimization problems of truss structures. These problems include a 10-bar planar truss, a 25-bar spatial truss, and a 220-bar transmission tower. 10-bar planar truss is solved considering continuous sizing variable. The other two examples are solved for both sizing and shape variable. The truss structures are analyzed using the direct stiffness method. The computations entailed by the MVSMCTS formulation and the direct stiffness method are performed in the Python software using Intel Core i7 2.30 GHz

processor and 40 GB memory.

4.1 Problem statement

The first example is the 10-bar planar truss shown in Fig. 11. This structure has been previously optimized by many researchers using a variety of techniques: harmony search (HS) (Lee and Geem 2004), PSO (Li et al. 2007), artificial bee colony (ABC) (Sonmez 2011), water evaporation optimization (WEO) (Kaveh and Bakhshpoori 2016), and political optimizer (PO) (Awad 2021).

The second test problem considers sizing and shape optimization of the 25-bar spatial truss shown in Fig. 12. This truss structure is previously designed by other methods such as GA (Wu and Chow 1995), PSO (Gholizadeh 2013), differential evolution (DE) (Ho-Huu et al. 2015), ABC (Jawad et al. 2021), and medalist learning algorithm (MLA) (He and Cui 2023).

The last example is the 220-bar transmission tower shown in Fig. 13. Various design parameters considered here are shown in Tables 2-9.

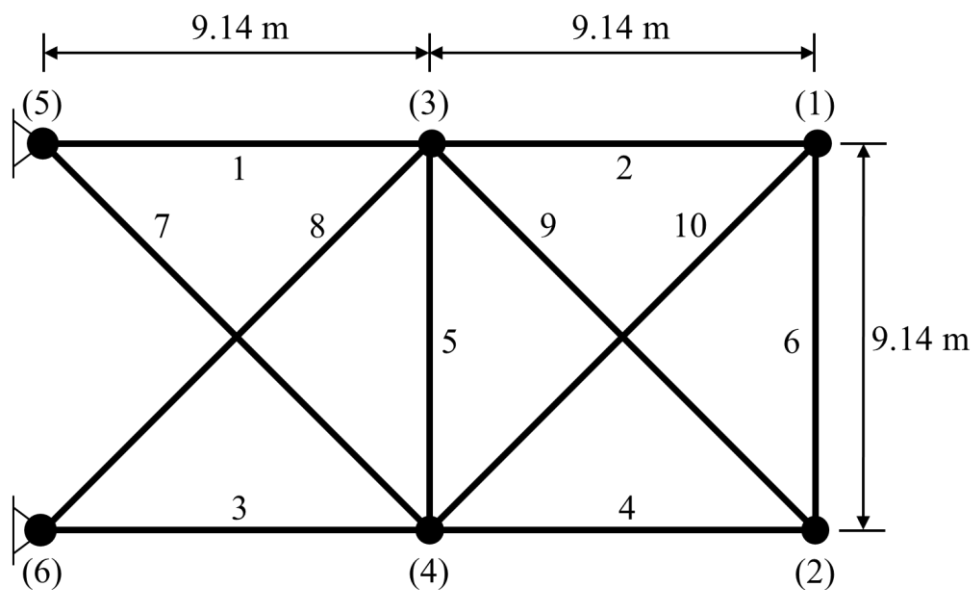


Fig. 11 Schematic of the 10-bar planar truss structure

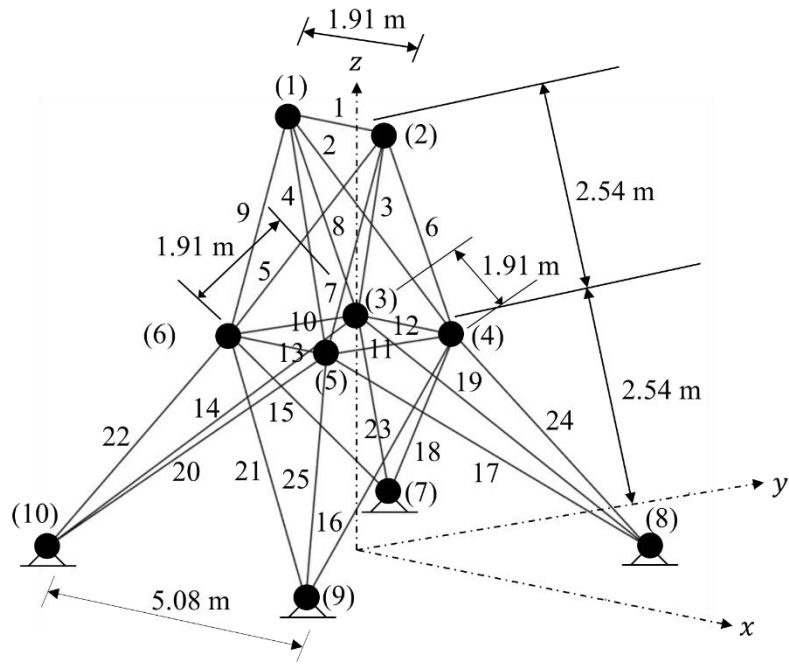


Fig. 12 Schematic of the 25-bar spatial truss structure

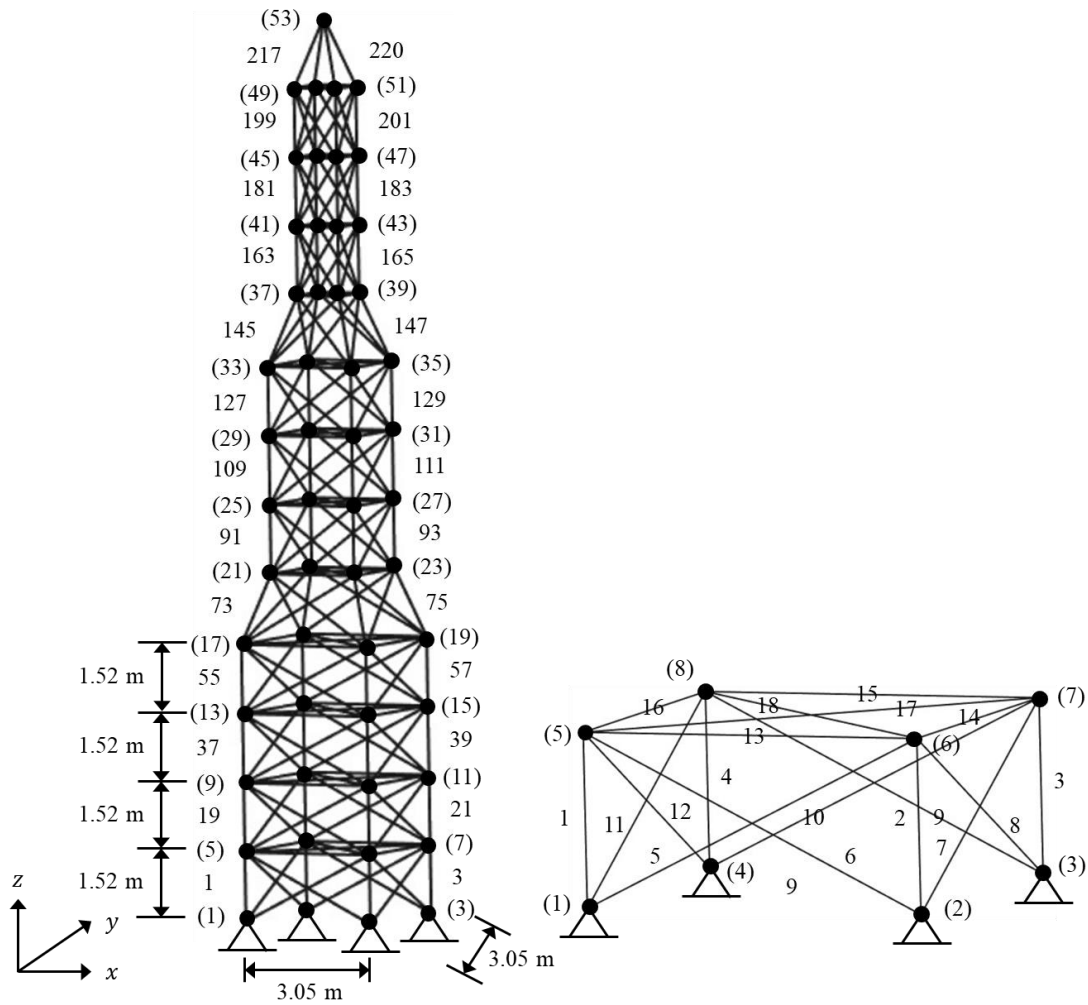


Fig. 13 Schematic of the 220-bar transmission tower

Table 2 Design consideration of the truss optimization problems

	10-bar planar truss	25-bar spatial truss	220-bar transmission tower
Design variables	$X_{i_X}, i_X = 1, 2, \dots, 10$	$X_{i_X}, i_X = 1, 2, \dots, 8$ $Y_{i_Y}, i_Y = 1, 2, \dots, 5$	$X_{i_X}, i_X = 1, 2, \dots, 49$ $Y_{i_Y}, i_Y = 1, 2, \dots, 21$
Material density (kg/m ³)	2767.99	2767.99	7860.00
Modulus of elasticity (GPa)	68.95	68.95	207.00
Stress limitation (MPa)	± 172.37	± 275.79	± 180.00
Displacement limitation (mm)	± 50.80	± 8.89	± 6.35
Load (kN)	$P_2^y = P_4^y = -444.82$	Table 4	Table 5

Table 3 Member grouping of the truss optimization problems

Truss problems	Member group
10-bar planar truss	No member group
25-bar spatial truss	25 truss members are grouped into 8 design variables, as follows: (1) 1, (2) 2-5, (3) 6-9, (4) 10-11, (5) 12-13, (6) 14-17, (7) 18-21, and (8) 22-25
220-bar transmission tower	Table 8

Table 4 Load case for the 25-bar spatial truss structure

Nodes k	Load case (kN)		
	P_k^x	P_k^y	P_k^z
1	4.45	-44.48	-44.48
2	0.00	-44.48	-44.48
3	2.22	0.00	0.00
6	2.67	0.00	0.00

Table 5 Load case for the 220-bar transmission tower

Nodes k	Load case 1 (kN)			Load case 2 (kN)		
	P_k^x	P_k^y	P_k^z	P_k^x	P_k^y	P_k^z
49	0.00	0.00	0.00	0.00	0.00	-400.00
50	0.00	0.00	0.00	0.00	0.00	-400.00
51	0.00	0.00	0.00	0.00	0.00	-400.00
52	0.00	0.00	0.00	0.00	0.00	-400.00
53	0.00	0.00	-2000.00	0.00	0.00	-400.00

Table 6 The lower and upper limit for sizing and shape

	10-bar planar truss	25-bar spatial truss
$X_{i_X, \min}$ (mm ²)	64.52	64.52
$X_{i_X, \max}$ (mm ²)	22582.00	2193.68
$Y_{i_Y, \min}$ (m)		$0.51 \leq x_4 = x_5 = -x_3 = -x_6 \leq 1.52$,
$Y_{i_Y, \max}$ (m)	N/A	$1.02 \leq y_3 = y_4 = -y_5 = -y_6 \leq 2.03$,
		$2.29 \leq z_3 = z_4 = z_5 = z_6 \leq 3.30$,
		$1.02 \leq x_8 = x_9 = -x_7 = -x_{10} \leq 2.03$,
		$2.54 \leq y_7 = y_8 = -y_9 = -y_{10} \leq 3.56$

220-bar transmission tower	
$X_{i_X, \min}$ (mm ²)	71.61
$X_{i_X, \max}$ (mm ²)	21612.86
$Y_{i_Y, \min}$ (m)	$-0.25 \leq x_5 = y_5 = y_6 = x_8 = x_9 = y_9 = y_{10} = x_{12} = x_{13} = y_{13} = y_{14} = x_{16} = x_{17} = y_{17} = y_{18} = x_{20} \leq 0.25,$ $2.79 \leq x_6 = x_7 = y_7 = y_8 = x_{10} = x_{11} = y_{11} = y_{12} = x_{14} = x_{15} = y_{15} = y_{16} = x_{18} = x_{19} = y_{19} = y_{20} \leq 3.30,$ $0.25 \leq x_{21} = y_{21} = y_{22} = x_{24} = x_{25} = y_{25} = y_{26} = x_{28} = x_{29} = y_{29} = y_{30} = x_{32} = x_{33} = y_{33} = y_{34} = x_{36} \leq 0.76,$ $2.29 \leq x_{22} = x_{23} = y_{23} = y_{24} = x_{26} = x_{27} = y_{27} = y_{28} = x_{30} = x_{31} = y_{31} = y_{32} = x_{34} = x_{35} = y_{35} = y_{36} \leq 2.79,$ $0.76 \leq x_{37} = y_{37} = y_{38} = x_{40} = x_{41} = y_{41} = y_{42} = x_{44} = x_{45} = y_{45} = y_{46} = x_{48} = x_{49} = y_{49} = y_{50} = x_{52} \leq 1.27,$ $1.78 \leq x_{38} = x_{39} = y_{39} = y_{40} = x_{42} = x_{43} = y_{43} = y_{44} = x_{46} = x_{47} = y_{47} = y_{48} = x_{50} = x_{51} = y_{51} = y_{52} \leq 2.29,$ $1.27 \leq x_{53} \leq 1.78, 1.27 \leq y_{53} \leq 1.78, 1.27 \leq z_5 = z_6 = z_7 = z_8 \leq 1.78, 2.79 \leq z_9 = z_{10} = z_{11} = z_{12} \leq 3.30,$ $4.32 \leq z_{13} = z_{14} = z_{15} = z_{16} \leq 4.83, 5.84 \leq z_{17} = z_{18} = z_{19} = z_{20} \leq 6.35, 7.34 \leq z_{21} = z_{22} = z_{23} = z_{24} \leq 7.87,$ $8.89 \leq z_{25} = z_{26} = z_{27} = z_{28} \leq 9.40, 10.41 \leq z_{29} = z_{30} = z_{31} = z_{32} \leq 10.92, 11.94 \leq z_{33} = z_{34} = z_{35} = z_{36} \leq 12.45,$ $13.46 \leq z_{37} = z_{38} = z_{39} = z_{40} \leq 13.97, 14.99 \leq z_{41} = z_{42} = z_{43} = z_{44} \leq 15.49, 16.51 \leq z_{45} = z_{46} = z_{47} = z_{48} \leq 17.02,$ $18.03 \leq z_{49} = z_{50} = z_{51} = z_{52} \leq 18.54, 19.56 \leq z_{53} \leq 20.07$

Table 7 Discrete set for sizing and shape

Truss problems	Discrete set
25-bar spatial truss	$D_{X, i_X} = \{0.65, 1.30, 1.95, \dots, 15.60, 16.25, 16.90, \dots, 22.10\}$ cm ² , $i_X = 1, 2, \dots, 8$
	$D_{Y, 1} = \{0.51, 0.57, 0.64, 0.70, \dots, 1.33, 1.40, 1.46, 1.52\}$ m
	$D_{Y, 2} = \{1.02, 1.08, 1.14, 1.21, \dots, 1.84, 1.91, 1.97, 2.03\}$ m
	$D_{Y, 3} = \{2.29, 2.35, 2.41, 2.48, \dots, 3.11, 3.18, 3.24, 3.30\}$ m
	$D_{Y, 4} = \{1.02, 1.08, 1.14, 1.21, \dots, 1.84, 1.91, 1.97, 2.03\}$ m
	$D_{Y, 5} = \{2.54, 2.60, 2.67, 2.73, \dots, 3.37, 3.43, 3.49, 3.56\}$ m
	D_{X, i_X} ($i_X = 1, 2, \dots, 49$) refers to Table 9.
	$D_{Y, 1} = \{-0.25, -0.22, -0.19, -0.16, \dots, 0.16, 0.19, 0.22, 0.25\}$ m
	$D_{Y, 2} = D_{Y, 10} = \{2.79, 2.83, 2.86, 2.89, \dots, 3.21, 3.24, 3.27, 3.30\}$ m
	$D_{Y, 3} = \{0.25, 0.29, 0.32, 0.35, \dots, 0.67, 0.70, 0.73, 0.76\}$ m
220-bar transmission tower	$D_{Y, 4} = \{2.29, 2.32, 2.35, 2.38, \dots, 2.70, 2.73, 2.76, 2.79\}$ m
	$D_{Y, 5} = \{0.76, 0.79, 0.83, 0.86, \dots, 1.17, 1.21, 1.24, 1.27\}$ m
	$D_{Y, 6} = \{1.78, 1.81, 1.84, 1.87, \dots, 2.19, 2.22, 2.25, 2.29\}$ m
	$D_{Y, 7} = D_{Y, 8} = D_{Y, 9} = \{1.27, 1.30, 1.33, 1.37, \dots, 1.68, 1.71, 1.75, 1.78\}$ m
	$D_{Y, 11} = \{4.32, 4.35, 4.38, 4.41, \dots, 4.73, 4.76, 4.79, 4.83\}$ m
	$D_{Y, 12} = \{5.84, 5.87, 5.91, 5.94, \dots, 6.25, 6.29, 6.32, 6.35\}$ m
	$D_{Y, 13} = \{7.37, 7.40, 7.43, 7.46, \dots, 7.78, 7.81, 7.84, 7.87\}$ m
	$D_{Y, 14} = \{8.89, 8.92, 8.95, 8.99, \dots, 9.30, 9.33, 9.37, 9.40\}$ m
	$D_{Y, 15} = \{10.41, 10.45, 10.48, 10.51, \dots, 10.83, 10.86, 10.89, 10.92\}$ m
	$D_{Y, 16} = \{11.94, 11.97, 12.00, 12.03, \dots, 12.35, 12.38, 12.41, 12.45\}$ m
	$D_{Y, 17} = \{13.53, 13.56, 13.59, 13.62, \dots, 13.87, 13.91, 13.94, 13.97\}$ m
	$D_{Y, 18} = \{14.99, 15.02, 15.05, 15.08, \dots, 15.40, 15.43, 15.46, 15.49\}$ m
$D_{Y, 19} = \{16.51, 16.54, 16.57, 16.61, \dots, 16.92, 16.95, 16.99, 17.02\}$ m	
$D_{Y, 20} = \{18.07, 18.10, 18.13, 18.16, \dots, 18.45, 18.48, 18.51, 18.54\}$ m	
$D_{Y, 21} = \{19.59, 19.62, 19.65, 19.69, \dots, 19.97, 20.00, 20.03, 20.07\}$ m	

Table 8 Member grouping of the 220-bar transmission tower

Number	Members	Number	Members	Number	Members	Number	Members
1	1-4	14	59-66	27	121-124	40	179-180
2	5-12	15	67-70	28	125-126	41	181-184
3	13-16	16	71-72	29	127-130	42	185-192
4	17-18	17	73-76	30	131-138	43	193-196
5	19-22	18	77-84	31	139-142	44	197-198
6	23-30	19	85-88	32	143-144	45	199-202
7	31-34	20	89-90	33	145-148	46	203-210
8	35-36	21	91-94	34	149-156	47	211-214
9	37-40	22	95-102	35	157-160	48	215-216
10	41-48	23	103-106	36	161-162	49	217-220
11	49-52	24	107-108	37	163-166		
12	53-54	25	109-112	38	167-174		
13	55-58	26	113-120	39	175-178		

Table 9 Discrete values available for cross-sectional areas from AISC norm

Number	Area (mm ²)	Number	Area (mm ²)	Number	Area (mm ²)	Number	Area (mm ²)
1	71.61	17	1008.39	33	2477.41	49	7419.34
2	90.97	18	1045.16	34	2496.77	50	8709.66
3	126.45	19	1161.29	35	2503.22	51	8967.72
4	161.29	20	1283.87	36	2696.77	52	9161.27
5	198.06	21	1374.19	37	2722.58	53	9999.98
6	252.26	22	1535.48	38	2896.77	54	10322.56
7	285.16	23	1690.32	39	2961.28	55	10903.20
8	363.23	24	1696.77	40	3096.77	56	12129.01
9	388.39	25	1858.06	41	3206.45	57	12838.68
10	494.19	26	1890.32	42	3303.22	58	14193.52
11	506.45	27	1993.54	43	3703.22	59	14774.16
12	641.29	28	2019.35	44	4658.06	60	15806.42
13	645.16	29	2180.64	45	5141.93	61	17096.74
14	792.26	30	2238.71	46	5503.22	62	18064.48
15	816.77	31	2290.32	47	5999.99	63	19354.80
16	940.00	32	2341.93	48	6999.99	64	21612.86

4.2 The effect of expansion of search region on the optimal solution for continuous sizing and shape variable

Figs. 14 and 15 illustrate the convergence histories for the 10-bar planar truss and the 25-bar spatial truss under different constants A_X and A_Y . It is worth mentioning that all design variables are continuous. The figures demonstrate that the proposed algorithm obtains the best solution when A_X and A_Y are all equal to 0.5. It indicates that the search region in each round must be expanded from the center.

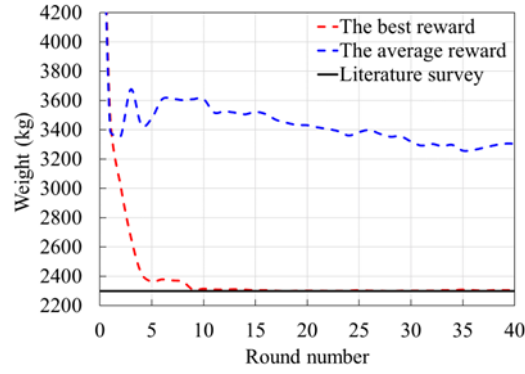


Fig. 14 Convergence histories for the 10-bar planar truss considering continuous sizing variable under different constant parameter A_X

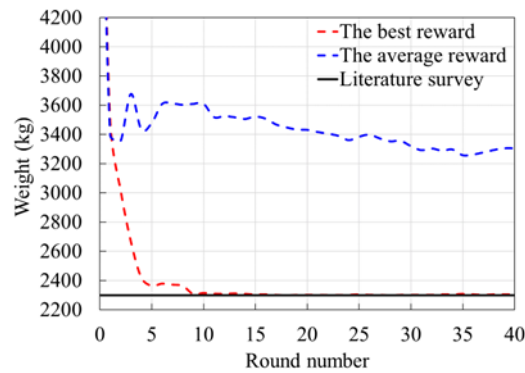


Fig. 15 Convergence histories for the 25-bar spatial truss considering continuous sizing and shape variable under different constant parameters A_X and A_Y

4.3 The effect of different types of accelerating techniques for continuous variable on the computation time

Table 10 compares the efficiency of IMCTS without and with different types of accelerating techniques based on CPU time. It can be seen that geometric decay is 1.5, 2.2, and 4.8 times faster than linear decrease, step reduction, and without accelerating technique.

Table 10. CPU time of IMCTS formulation without and with different types of accelerating techniques

	Without accelerating technique	Geometric decay	Linear decrease	Step reduction
10-bar planar truss (Case 1)	223.49 sec	46.53 sec	62.94 sec	102.47 sec
10-bar planar truss (Case 2)	380.13 sec	86.02 sec	102.45 sec	264.03 sec
72-bar spatial truss (Case 1)	12749.90 sec	2549.98 sec	3470.55 sec	4978.25 sec
72-bar spatial truss (Case 2)	36154.62 sec	8408.05 sec	14851.48 sec	20872.75 sec

4.4. Investigation of convergence history: 10-bar planar truss

Figure 18 illustrates the comparison of convergence histories for the 10-bar planar truss under the best and average reward. Figure 18(a) and (b) for Case 1 and Case 2 demonstrates that the proposed method obtains the best solution at 13 and 15 rounds under the best reward. However, this method does not detect the best solution after 40 rounds under the average reward.

The comparison of convergence histories for the 10-bar planar truss under different parameter α is shown in Figure 19. From Figure 19(a) and (b), this algorithm obtains the best solution at 13 and 18 rounds under minimum weight for Case 1 and Case 2. However, for Case 1 and Case 2, this algorithm does not detect the best solution after 40 rounds under maximum weight.

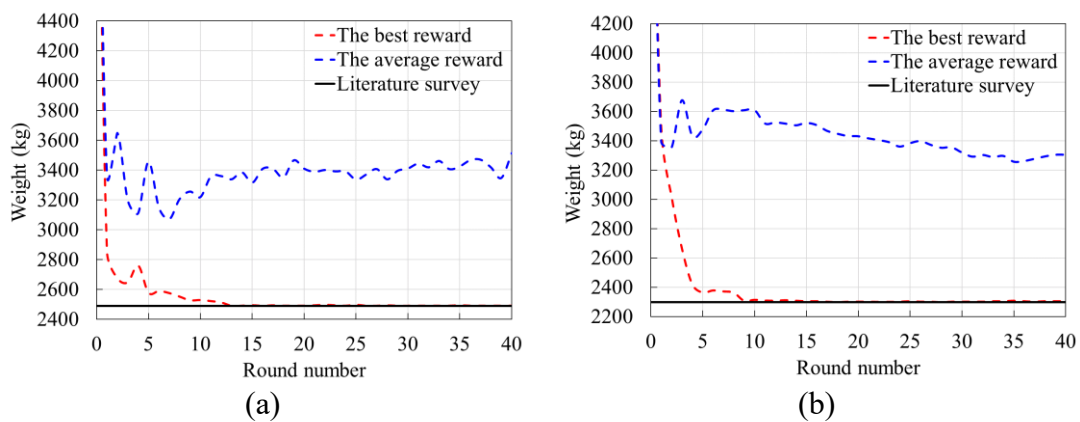


Figure 18. Comparison of the convergence histories for 10-bar planar truss under the best and average reward for (a) Case 1 and (b) Case 2.

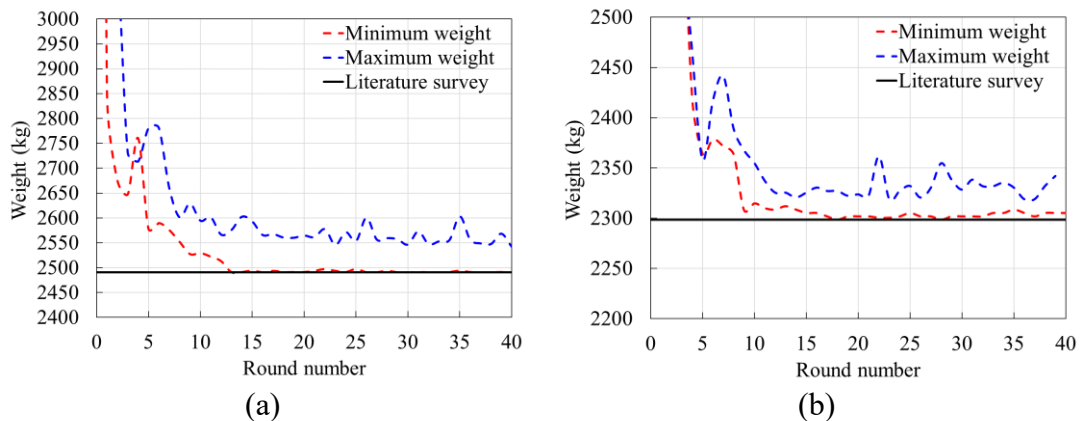


Figure 19. Comparison of the convergence histories for 10-bar planar truss under parameter α equal to minimum and maximum weight for (a) Case 1 and (b) Case 2.

4.5 Solution accuracy

Three truss optimization problems, including a 15-bar planar truss, a 25-bar spatial truss, and a 220-bar transmission tower are used to validate the solution accuracy by comparing the results which have been previously investigated by other researchers.

Tables 9-10 demonstrate the comparison of optimal design results for a 15-bar planar truss and a 25-bar spatial truss. It is shown that the IMCTS formulation outperforms all metaheuristic algorithms in terms of the lightest weight. Optimal layouts after the optimization with the IMCTS formulation are given in Figs. 15-17. Figs. 18-20 indicate that the optimal solution assessed by the IMCTS formulation does not violate normal stresses and nodal displacement constraints.

Table 10 Comparison of optimal designs for the 25-bar spatial truss structure

Design variables	GA	PSO	FA	DE	ABC	UMCTS
Sizing optimization/Cross-sectional area (mm²)						
1	0.65	0.65	0.65	0.65	0.65	0.65
2-5	1.30	0.65	0.65	0.65	0.65	0.65
6-9	7.15	7.15	5.85	5.85	6.45	6.50
10-11	1.30	0.65	0.65	0.65	0.65	0.65
12-13	1.95	2.60	0.65	0.65	0.65	0.65
14-17	0.65	0.65	0.65	0.65	0.65	0.65
18-21	1.30	2.60	0.65	0.65	0.65	0.65
22-25	5.85	4.55	6.45	6.45	5.85	5.85
Shape optimization/Nodal coordinate (mm)						
x_4	1.04	0.70	0.95	0.94	0.92	0.95
y_3	1.36	1.31	1.42	1.49	1.39	1.39
z_3	3.16	3.30	3.22	3.12	3.30	3.29
x_8	1.29	1.08	1.27	1.25	1.32	1.30
y_7	3.34	3.37	3.46	3.47	3.56	3.49
Weight (kg)	61.78	58.61	53.90	53.87	53.22	52.96

Table 11 Optimal design for 220-bar transmission tower

Sizing optimization							
Number	Cross-sectional area (mm ²)	Number	Cross-sectional area (mm ²)	Number	Cross-sectional area (mm ²)	Number	Cross-sectional area (mm ²)
1	8709.66	14	71.61	27	71.61	40	90.97
2	71.61	15	198.06	28	71.61	41	7419.34
3	90.97	16	1858.06	29	8709.66	42	71.61
4	1690.32	17	8967.72	30	71.61	43	71.61
5	8967.72	18	71.61	31	641.29	44	71.61
6	71.61	19	1161.29	32	2180.64	45	7419.34
7	90.97	20	645.16	33	8709.66	46	71.61
8	71.61	21	8709.66	34	90.97	47	1690.32
9	8709.66	22	71.61	35	494.19	48	252.26
10	90.97	23	71.61	36	2503.22	49	8709.66
11	90.97	24	71.61	37	8709.66		
12	161.29	25	8967.72	38	71.61		
13	9161.27	26	71.61	39	90.97		
Shape optimization							
Number	Nodal coordinate (mm)	Number	Nodal coordinate (mm)	Number	Nodal coordinate (mm)	Number	Nodal coordinate (mm)
1	242.09	7	1492.16	13	7866.06	19	16545.712
2	2797.97	8	1491.10	14	9178.75	20	18085.15
3	612.50	9	1695.93	15	10414.00	21	19563.95
4	2399.00	10	2951.43	16	11938.00		
5	1137.09	11	4353.72	17	13966.03		
6	1861.70	12	5842.00	18	15387.90		

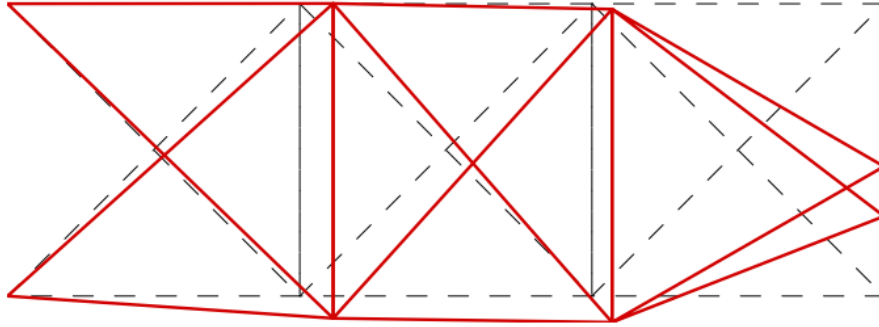


Fig. 15 15-bar planar truss structure: comparison of the optimized layout with the initial configuration of the truss

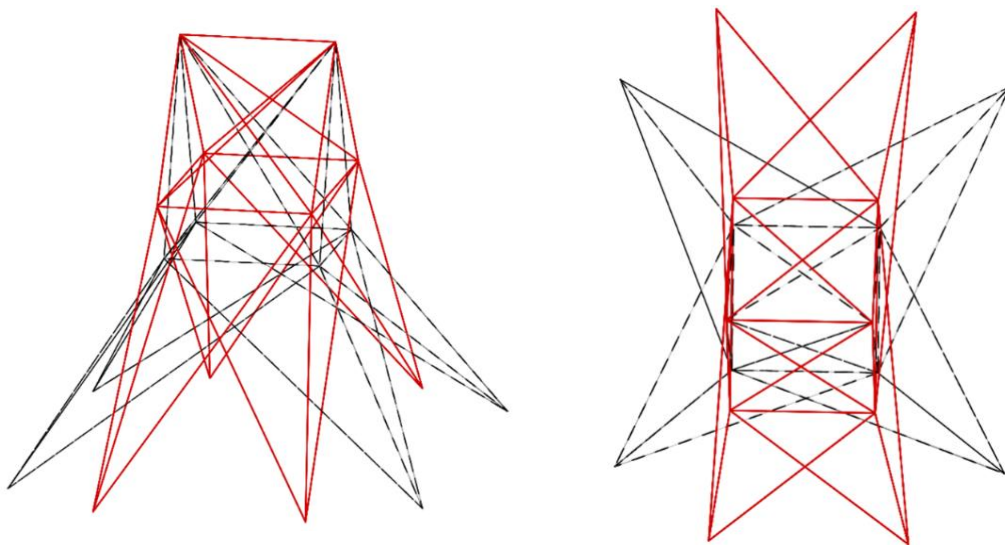


Fig. 16 25-bar spatial truss structure: comparison of the optimized layout with the initial configuration of the truss

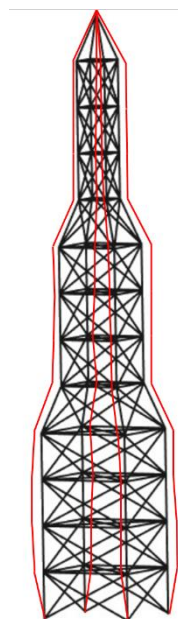


Fig. 17 220-bar transmission tower: comparison of the optimized layout with the initial configuration of the truss

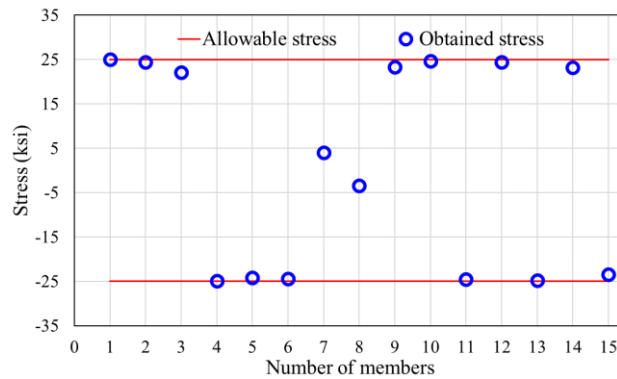


Fig. 18 Constraints boundaries assessed at the optimal design of 15-bar planar truss structure by the IMCTS formulation

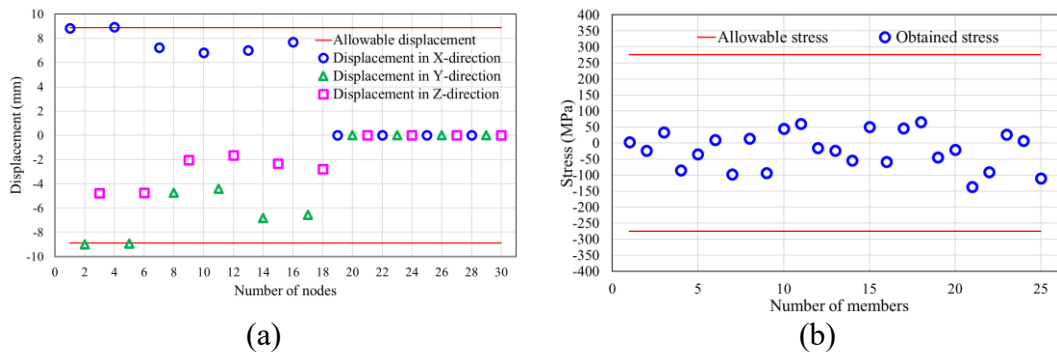


Fig. 19 Constraints boundaries assessed at the optimal design of 25-bar spatial truss structure by the IMCTS formulation for (a) displacement constraints (b) stress constraints

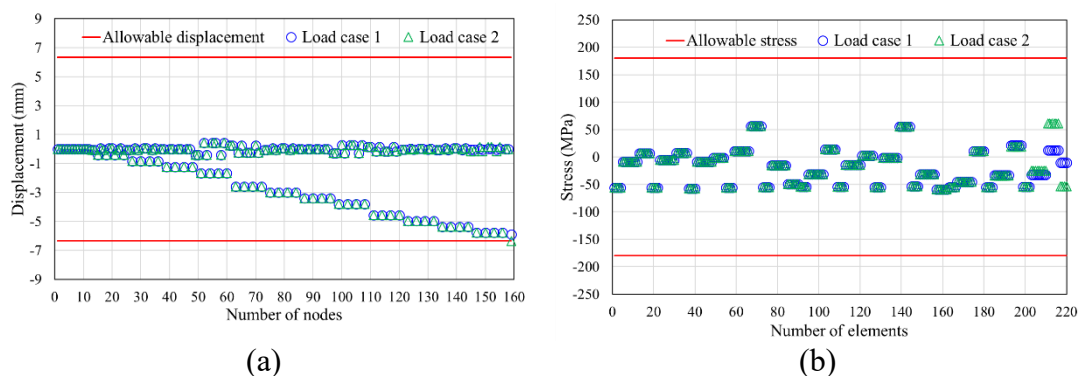


Fig. 20 Constraints boundaries assessed at the optimal design of 220-bar transmission tower by the IMCTS formulation for (a) displacement constraints (b) stress constraints

4.4 Solution stability

The statistical results for 15-bar planar truss, 25-bar spatial truss, and 220-bar transmission tower are obtained through 10 independent sampling to test the stability

of this algorithm. The results are shown in Table 12, including the best, the worst, average, and standard deviation.

Table 12 Statistical results of the investigated example

Investigated example	Best weight	Worst weight	Average weight	Standard deviation
15-bar planar truss	34.40 kg	36.39 kg	35.66 kg	0.59
25-bar spatial truss	53.16 kg	56.91 kg	54.24 kg	1.02
220-bar transmission tower	6113.64 kg	6302.15 kg	6226.99 kg	76.98

5 Summary and conclusions

In this paper, an RL algorithm using MVSMCTS formulation is developed to solve optimization problems considering various types of variables with single and mixed system. MVSMCTS formulation is based on IMCTS formulation for discrete sizing optimization. Sizing and shape optimization of truss structures is utilized as an example for mixed variable structural optimization. For this problem, the design variables are the cross-sectional areas of the members and the nodal coordinates of the joints. It is difficult to find an optimal solution in a reasonable time because various types of variables are of fundamentally different nature. The following conclusions are obtained:

- (1) The computational framework of update process for discrete variable is also suitable for continuous variable. In order to adopt update process in continuous space, uniform meshes are generated automatically in search region.
- (2) For continuous variable, the search region in each round should be expanded from the center, which is the design variable for initial state.
- (3) Accelerating technique for continuous variable incorporates decreasing the range of search region and the width of search tree as the update process proceeds. The width of search tree is based on the number of meshes generated in each round.
- (4) Three kinds of accelerating techniques including geometric decay, linear decrease, and step reduction are also considered for continuous variable. Regardless of the range of search region and the width of search tree, geometric decay performs better than linear decrease and step reduction related to computational cost.
- (5) For MVSMCTS formulation, various types of variables are considered in only one search tree.
- (6) MDP framework, four steps of MCTS, UCB, the best reward, policy improvement, update process and accelerating technique for discrete variable and terminal condition in IMCTS formulation can also be employed in MVSMCTS formulation.

The proposed algorithm allows the agent to find an optimal solution. The numerical examples demonstrate that this algorithm provides results as good as metaheuristic algorithms in a reasonable time and applicable for practical engineering problems. In conclusion, this study suggests that MVSMCTS formulation is a powerful optimization

technique for mixed variable structural optimization without tuning parameters.

The proposed method is expected to solve more complex problems such as simultaneous sizing, shape, and topology optimization of truss structures, which are our future research interests.

References

- Browne CB, Powley E, Whitehouse D, Lucas SM, Cowling PI, Rohlfshagen P, Tavener S, Perez D, Samothrakis S, Colton S (2012) A survey of Monte Carlo tree search methods. *IEEE Trans Comput Intell AI Games* 4 (1): 1-43. [10.1109/TCIAIG.2012.2186810](https://doi.org/10.1109/TCIAIG.2012.2186810)
- Dede T, Ayvaz Y (2015) Combined size and shape optimization of structures with a new meta-heuristic algorithm. *Appl Soft Comput* 28: 250-258. <https://doi.org/10.1016/j.asoc.2014.12.007>
- Ding Y (1986) Shape optimization of structures: A literature survey. *Comput Struct* 24 (6): 985-1004. [https://doi.org/10.1016/0045-7949\(86\)90307-X](https://doi.org/10.1016/0045-7949(86)90307-X)
- Gholizadeh S (2013) Layout optimization of truss structures by hybridizing cellular automata and particle swarm optimization. *Comput Struct* 125: 86-99. <https://doi.org/10.1016/j.compstruc.2013.04.024>
- Hansen SR, GN Vanderplaats (1990) Approximation method for configuration optimization of trusses. *AIAA J* 28 (1): 161-168. <https://doi.org/10.2514/3.10367>
- Hayashi K, Ohsaki M (2020) Reinforcement learning and graph embedding for binary truss topology optimization under stress and displacement constraints. *Front Built Environ* 6: 59. <https://doi.org/10.3389/fbuil.2020.00059>
- Hayashi K, Ohsaki M (2021) Reinforcement learning for optimum design of a plane frame under static loads. *Eng Comput* 37: 1999-2011. <https://doi.org/10.1007/s00366-019-00926-7>
- Hayashi K, Ohsaki M (2022) Graph-based reinforcement learning for discrete cross-section optimization of planar steel frames. *Adv Eng Inform* 51: 101512. <https://doi.org/10.1016/j.aei.2021.101512>
- He SX, Cui YT (2023) Medalist learning algorithm for configuration optimization of trusses. *Appl Soft Comput* 148: 110889. <https://doi.org/10.1016/j.asoc.2023.110889>
- Ho-Huu V, Nguyen-Thoi T, Nguyen-Thoi MH, Le-Anh L (2015) An improved constrained differential evolution using discrete variables (D-ICDE) for layout optimization of truss structures. *Expert Syst Appl* 42 (20): 7057-7069. <https://doi.org/10.1016/j.eswa.2015.04.072>
- Jawad FKJ, Ozturk C, Dansheng W, Mahmood M, Al-Azzawi O, Al-Jemely A (2021) Sizing and layout optimization of truss structures with artificial bee colony algorithm. *Structures* 30: 546-559. <https://doi.org/10.1016/j.istruc.2021.01.016>

- Kaveh A, Kalatjari V (2004) Size/geometry optimization of trusses by the force method and genetic algorithm. *ZAMM-Z Angew Math Mech* 84 (5): 347-357. <https://doi.org/10.1002/zamm.200310106>
- Kaveh A, Mirzaei B, Jafarvand A (2015) An improved magnetic charged system search for optimization of truss structures with continuous and discrete variables. *Appl Soft Comput* 28: 400-410. <https://doi.org/10.1016/j.asoc.2014.11.056>
- Kirsch U, Topping BHV (1992) Minimum weight design of structural topologies. *J Struct Eng* 118 (7): 1770-1785. [https://doi.org/10.1061/\(ASCE\)0733-9445\(1992\)118:7\(1770\)](https://doi.org/10.1061/(ASCE)0733-9445(1992)118:7(1770))
- Ko FY, Suzuki K, Yonukura K (2024) Improved Monte Carlo tree search formulation with multiple root nodes for discrete sizing optimization of truss structures. arXiv:2309.06045. <https://doi.org/10.48550/arXiv.2309.06045>
- Kupwiwat C, Hayashi K, Ohsaki M (2023) Deep deterministic policy gradient and graph attention network for geometry optimization of latticed shells. *Appl Intell* 53: 19809-19826. <https://doi.org/10.1007/s10489-023-04565-w>
- Lee KS, Geem ZW (2004) A new structural optimization method based on the harmony search algorithm. *Comput Struct* 82 (9-10): 781-798. <https://doi.org/10.1016/j.compstruc.2004.01.002>
- Li LJ, Huang ZB, Liu F, Wu QH (2007) A heuristic particle swarm optimizer for optimization of pin connected structures. *Comput Struct* 85 (7-8): 340-349. <https://doi.org/10.1016/j.compstruc.2006.11.020>
- Lipson SL, Gwin LB (1977) The complex method applied to optimal truss configuration. *Comput Struct* 7 (3): 461-468. [https://doi.org/10.1016/0045-7949\(77\)90083-9](https://doi.org/10.1016/0045-7949(77)90083-9)
- Luo R, Wang Y, Liu Z, Xiao W, and Zhao X (2022b) A reinforcement learning method for layout design of planar and spatial trusses using Kernel Regression 12 (16): 8227. <https://doi.org/10.3390/app12168227>
- Luo R, Wang Y, Xiao W, Zhao X (2022a) AlphaTruss: Monte Carlo tree search for optimal truss layout design. *Buildings-Basel* 12 (5): 641. <https://doi.org/10.3390/buildings12050641>
- Miguel LFF, Lopez RH, Miguel LFF (2013) Multimodal size, shape, and topology optimisation of truss structures using the Firefly algorithm. *Adv Eng Softw* 56: 23-37. <https://doi.org/10.1016/j.advengsoft.2012.11.006>
- Ororbia M, Warn GP (2022) Design synthesis through a Markov Decision Process and reinforcement learning framework. *J Comput Inf Sci Eng* 22 (2): 021002. <https://doi.org/10.1115/1.4051598>
- Sonmez M (2011) Artificial bee colony algorithm for optimization of truss structures. *Appl Soft Comput* 11 (2): 2406-2418. <https://doi.org/10.1016/j.asoc.2010.09.003>

s

Topping B (1983) Shape optimization of skeletal structures: A review. *J Struct Eng* 109 (8): 1933-1951. [https://doi.org/10.1061/\(ASCE\)0733-9445\(1983\)109:8\(1933\)](https://doi.org/10.1061/(ASCE)0733-9445(1983)109:8(1933))

Vanderplaats GN, Moses F (1972) Automated design of trusses for optimum geometry. *J Struct Div* 98 (3): 671-690. <https://doi.org/10.1061/JSDEAG.0003181>

Wu SJ, Chow PT (1995) Integrated discrete and configuration optimization of trusses using genetic algorithms. *Comput Struct* 55 (4): 695-702. [https://doi.org/10.1016/0045-7949\(94\)00426-4](https://doi.org/10.1016/0045-7949(94)00426-4)

Zhou M, R Xia (1990) An efficient method of truss design for optimum geometry *Comput Struct* 35 (2): 115-119. [https://doi.org/10.1016/0045-7949\(90\)90331-U](https://doi.org/10.1016/0045-7949(90)90331-U)

Publisher's note Springer Nature remains neutral with regard to jurisdictional claims in published maps and institutional affiliations.